ACKNOWLEDGEMENT

The writer wishes to express his sincere thanks to his supervisor, Dr. Z.A. Zielinski, for his help and guidance, as well as for his encouragement and valuable advice during the course of this study and the writing of this thesis.

Grateful acknowledgement is made to Miron Inc. in Montreal for the provision of ready-mixed concrete.

The author is indebted to the technical staff of the Civil Engineering Laboratory for instrumentation and for help in carrying out measurements. Many thanks are especially due to Boon Ting Phoa, an undergraduate student in the Department of Civil Engineering for his help in preparing specimens and in conducting the tests.

TABLE OF CONTENTS

LIST OF FIGURES

Figure — Page

LIST OF TABLES

NOTATIONS

α = ratio of relative tensile strength f_t to uniaxial compressive strength f_c'

b = flange width in a T-section, as defined in Fig. 20a

b' = web thickness in a T-section, as defined in Fig. 20a

d = diameter of a concrete cylinder

d' = flange thickness in a T-section, as defined in Fig. 20a

ε_b^t = tensile strain in biaxial loading

ε_{cc} = concrete compressive strain in the extreme fiber, as defined in Fig. 20c

ε_{ct} = concrete tensile strain in the extreme fiber, as defined in Fig. 20c

ε_u^+ = tensile strain in uniaxial loading

E_c = concrete modulus of elasticity

f_c' = compressive strength of concrete

f_{cc} = concrete compressive stress in the extreme fiber, as defined in Fig. 20b

f_{ct} = compressive strength of concrete under combined bi-directional compression and tension

f_t' = concrete cylinder splitting strength

$f_{t(-)}$ = tensile strength in one-way specimen

f_t^b = biaxial tensile strength in two-way specimen

f_{tc} = tensile strength of concrete under combined bi-directional tension and compression

f_{to} = uniaxial tensile strength of concrete

f_t = relative tensile strength of concrete, depending upon specimen and loading type

f_{tt} = biaxial tensile strength of concrete

$f^{u}_{t(+)}$ = uniaxial tensile strength in two-way specimen

h = overall depth of a T-section, as defined in Fig. 20a

L = concrete cylinder length

λ = plasticity coefficient

M_{cr} = ultimate moment capacity of plain concrete

P = applied concentrated load

P_u = applied concentrated load at failure

P^{b}_{u} = applied concentrated load at failure in biaxial loading

P^{u}_{u} = applied concentrated load at failure in uniaxial loading

W = specific weight of concrete

x = distance from neutral axis to the extreme compressive fiber

INTRODUCTION

In many structures such as plates, shells, various containment structures, concrete tension membrane roofs, ribbed panel structures, or even waffle like systems, concrete is subjected to multidirectional stress. Little attention is given to multiaxial strength of concrete in present recommended design practices. In fact, most structural designs are based on uniaxial strength, even where working conditions cause combined stress states. Such simplification can be acceptable for locations under multidirectional compression since, as it well known, strength of concrete is higher in multiaxial compression. However, there is not enough data to justify such simplification for multiaxial tension which may have significant consequences on structures such as those mentioned above.

At the present time, there is available ample experimental data for the combined stress conditions of compression-compression and compression-tension. However, only limited test data are available for biaxial tension, and results obtained by various researchers deviate from each other.

One of the major problems in conducting tests on concrete subjected to biaxial stresses is the development of a well-defined unobstructed uniform biaxial stress state in the specimen. Discrepancies between available test results often are due to differences in the stress state developed in test specimens.

A BRIEF REVIEW OF LITERATURE

The strength of concrete subject to biaxial states of stress has been under investigation for the past seventy years. The research in this area can be divided into three categories, depending on the type of specimen used.

Richart, Brandtzaeg, and Brown[1] used a cylindrical specimen to study the behaviour of concrete in bi-directional compression. In this investigation, a cylinder was loaded longitudinally and was subjected at the same time to hydrostatic pressure in radial directions. The investigators admitted that in order to develop a truly biaxial stress state, restraint of the cylinders at the top and bottom should be avoided, and penetration of the pressure fluid into cracks or pores on the surface of the concrete should be prevented. Realizing that both of these requirements may not have been fully satisfied, the investigators limited their conclusion to the statement that the strength of concrete in two dimensional compression was at least as great as the strength in simple compression, and in most cases, it was greater. The ultimate failure occurred by a sudden fracture of the specimen into two parts along a plane approximately normal to the axis of the cylinder.

To study the behaviour of concrete under combined compressive and tensile stresses, Bresler and Pister[2], Goode and Helmy[3], McHenry and Karni[4], used hollow cylinders subjected either to torsion and axial compression or to internal hydraulic pressure and axial compression. Large ratios of wall thickness to diameter of the specimen may lead to noticeable deviations from a uniform stress distribution across the thickness of the cylinder. However, the results from the various inves-

tigations are in comparatively good agreement and give a clear indication of the linear behaviour of concrete subjected to a combination of tensile and compressive stresses. Bellamy[5] used hollow cylinders subjected to external pressure and axial compression. Values of the biaxial compressive strength up to 2.69 times the uniaxial strength were recorded.

Concrete plates were used for studies of biaxial strength over the entire range of stress combinations by Tasuji, Slate, and Nilson[6], Kupfer, Hilsdorf, and Rüsch[7], Liu, Nilson, and Slate[8], Carino and Slate[9]. Plates were loaded without restraint by replacing the solid bearing platens of a conventional testing machine with filaments in the form of "brush bearing platens". These platens consist of a series of closely-spaced small steel bars which are flexible enough to follow the concrete deformations without generating significant restraint in the test sample. For tensile tests the filaments can be glued to the concrete. The results of the above-mentioned investigators are in very good agreement over the combined stress conditions of compression-compression and compression-tension. It is concluded that the ultimate strength of concrete in biaxial compression is greater than in uniaxial (maximum strength increases of approximately 22 to 27 percent). Under biaxial compression-tension, the compressive strength decreases almost linearly as the applied tensile stress is increased. Tasuji *et al.*[6] and Kupfer, *et al.*[7], on the basis of their tests, have noticed increase and no change respectively, in biaxial tensile strength as compared with uniaxial. They have also measured strains in the three principal directions of tested concrete plates and have found that in uniaxial and biaxial compression, the compressive strain at maximum

load was about -2500 microstrain; in uniaxial and biaxial tension, the tensile strain at maximum load was about +150 microstrain.

Figure 1-0 shows experimental biaxial ultimate strength envelopes obtained from various sources.

RESEARCH OBJECTIVE

The objective of this research was to develop a simple test model and to produce more data on biaxial tensile strength of concrete in relation to uniaxial, and to compare the results with those of other researchers.

In this investigation, a new test specimen is introduced which appears to be simple enough and appropriate for comparable definition of flexural tensile strength of concrete in uniaxial and biaxial loading.

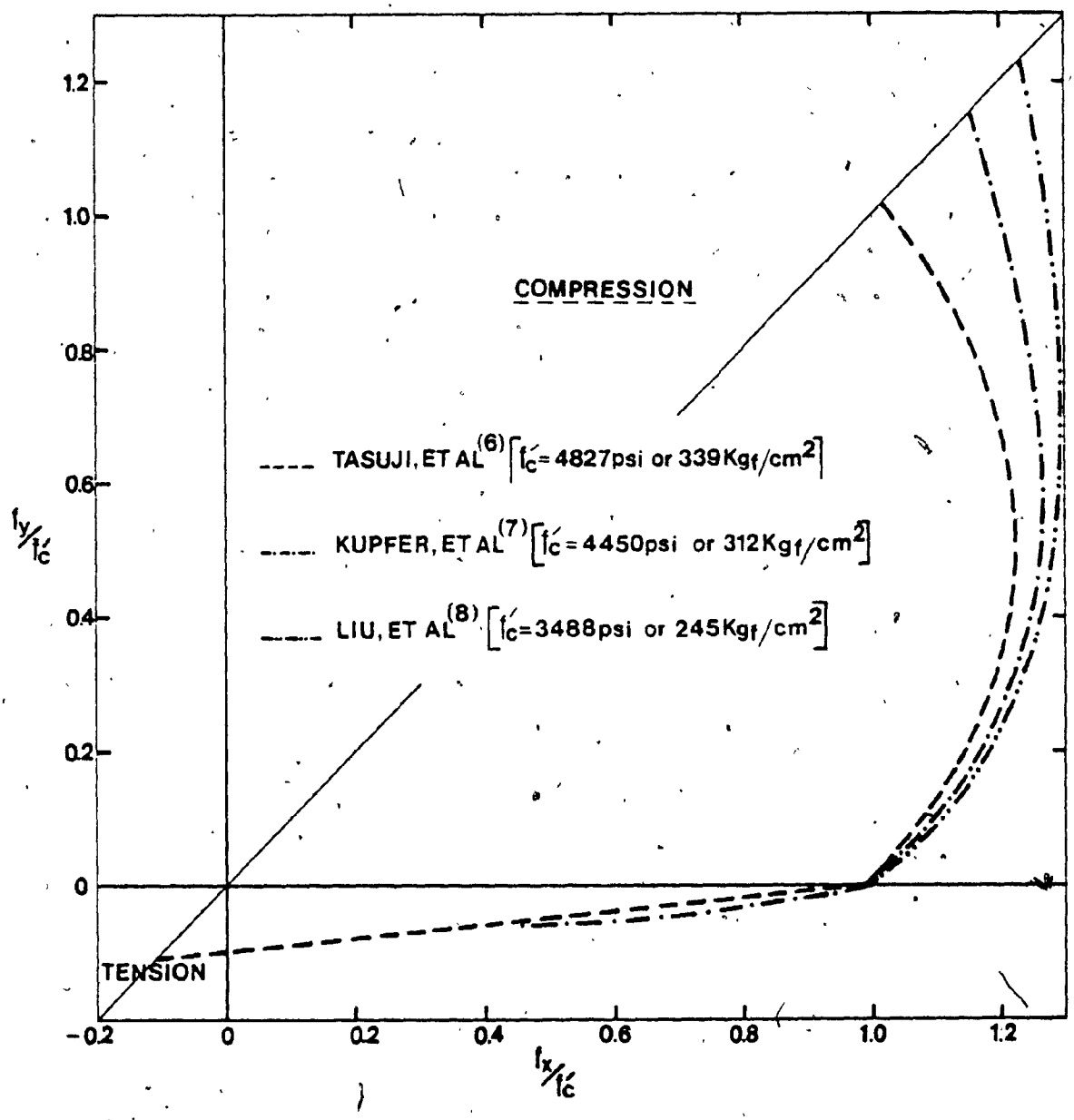

Fig. 1-0 Experimental biaxial ultimate strength envelopes obtained from various sources

INVESTIGATION PROGRAM

The test program included:

(1) One-way ribbed slab specimens subjected to uniaxial tension and

(2) Two-way ribbed slab specimens subjected to uniaxial and biaxial tension.

The specimens represented part of a waffle-like structure (Fig. 1) and consisted of thin slab and deep ribs. The slab was 2 in (50.8 mm) thick with a width varying from 24 in (609.6 mm) in the centre to 4.00 in (101.6 mm) at the ends. The ribs were 6 in (152.4 mm) deep and 3 in (76.2 mm) wide.

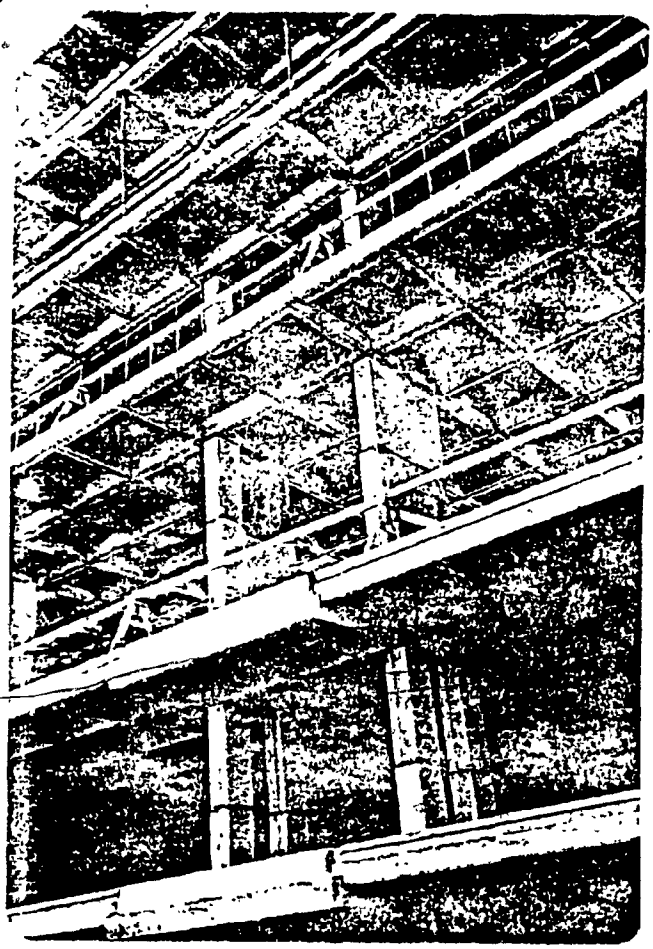

Fig. 1 Waffle-like floor system on Terrace Inn complex in Edmonton (Structural design by Z.A. Zielinski)

In total, 30 specimens grouped in 5 series were tested. The test series, except No. 5, each contained 6 two-way ribbed specimens (Fig. 2) of which 3 were tested uniaxially and 3 biaxially. Series No. 5 consisted of 3 one-way (Fig. 3) and 3 two-way ribbed specimens, all tested uniaxially.

Each test series was accompanied by 3 control cylinders 6 x 12 in (15x30cm), tested in uniaxial compression for the determination of the standard

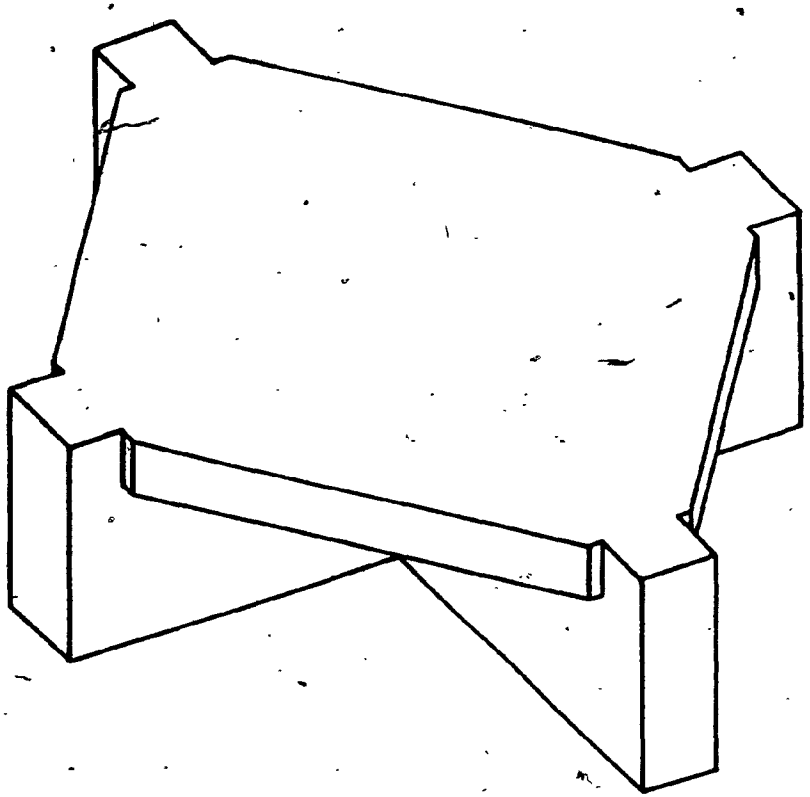

(a) Axisymmetric view

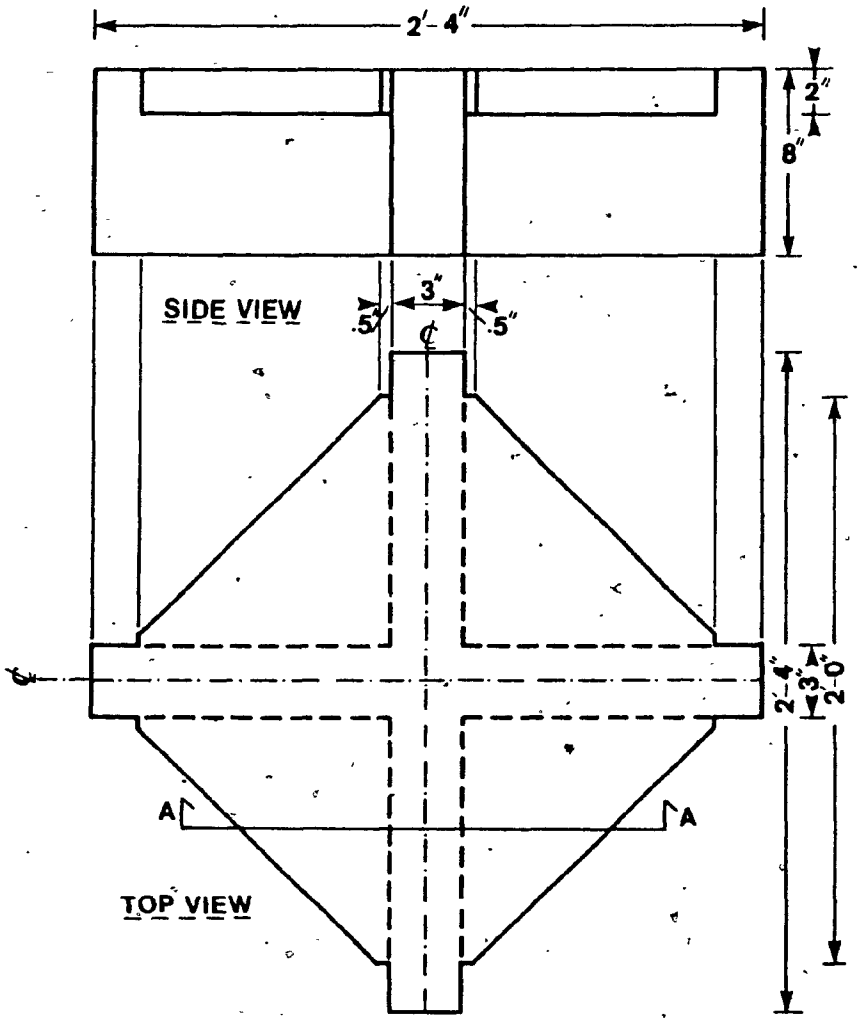

(b) Top view, side view and cross section

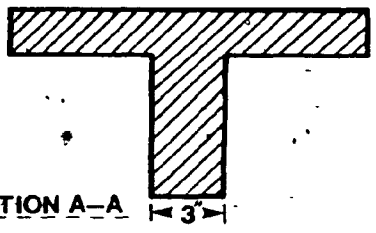

Fig. 2 Two-way ribbed slab specimen

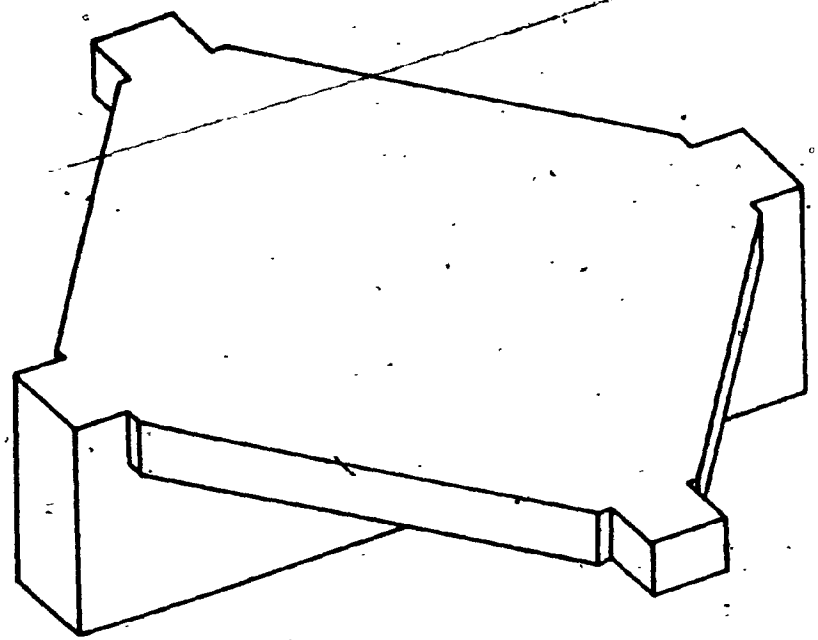

(a) Axisymmetric view

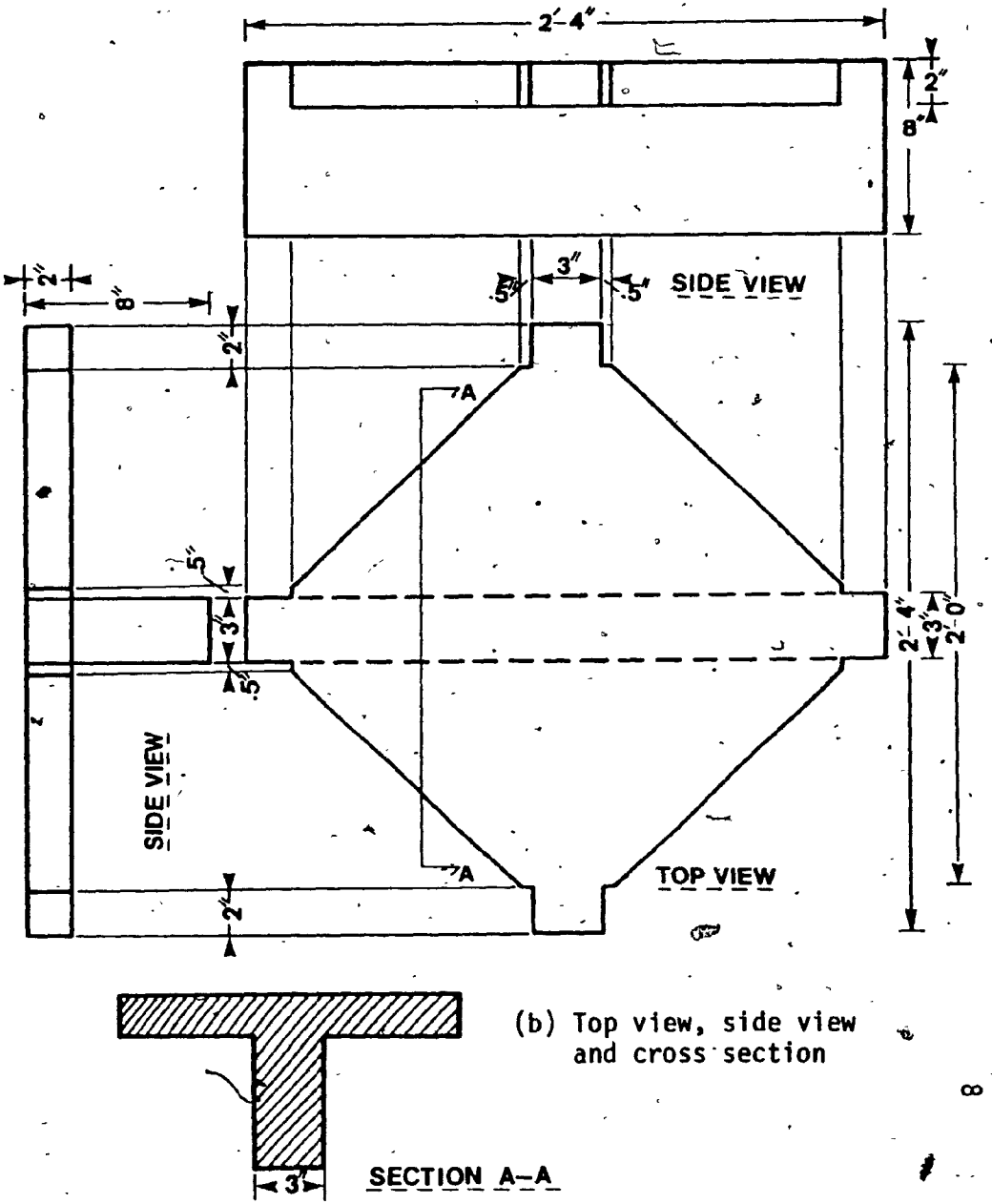

(b) Top view, side view and cross section

Fig. 3 One-way ribbed slab specimen

uniaxial compressive strength f'_c (results are shown in Table 1). In addition, test series No. 3 and 5 were accompanied by split cylinder tests (6 cylinders for series No. 3 and 3 for series No. 5).

The specimens were made out of plain ready-mixed concrete provided by Miron Inc. Five types of concrete with an uniaxial compressive strength of 3430, 3830, 3720, 4020, 4350 psi (23.66, 26.41, 25.66, 27.72, 30.0 MPa) were tested. Type 10 normal cement was used and gravel with maximum aggregate size of 20 mm (0.8 in). The water-cement ratio for the first four types of concrete was 0.71, 0.63, 0.45, 0.37 respectively. The sand-cement ratio was 0.23, 0.32, 0.44, 0.61 and the aggregate-cement ratio 0.25, 0.25, 0.37, 0.46 respectively.

The specimens were cast in wooden forms (Fig. 4) and the cylinders in standard plastic impervious molds. A single reinforcing bar of 0.125 in (3 mm) in diameter was placed in compression zone of the sample along the perimeter of the slab, as shown in Fig. 5, for structural purpose (handling strength).

Fig. 4 Specimen Formwork

Concrete was compacted with a vibrator. Samples were removed from molds after 3 days and then stored in the laboratory under controlled conditions (temperature of 72F (22C) and relative humidity of 65 percent until time of test.

Before testing, electric strain gauges of the type CEA-06-250UW-120 from Vishay Intertechnology Inc., were attached to the bottom

TABLE 1. COMPRESSION TEST RESULTS OF CONTROL CYLINDERS

SERIES NO	CYLINDER DESIGNATION	LOAD AT FAILURE lbs (KN)	AVERAGE LOAD AT FAILURE lbs (KN)	SERIES COMPRESSIVE STRENGTH f'_c psi (MPa)
(1)	(2)	(3)	(4)	(5)
1	20/1	97,600(434.2)	96,933(431.3)	3430(23.66)
	20/2	92,800(412.9)		
	20/3	100,400(446.7)		
2	25/1	112,000(498.5)	108,333(482.0)	3830(26.41)
	25/2	110,000(489.4)		
	25/3	103,000(458.2)		
3	30/1	101,500(451.6)	105,083(467.5)	3720(25.66)
	30/2	96,800(430.7)		
	30/3	104,800(466.3)		
	30/4	118,000(525.0)		
	30/5	100,000(444.9)		
	30/6	100,400(486.7)		
4	35/1	120,000(533.9)	113,667(505.7)	4020(27.72)
	35/2	112,000(498.3)		
	35/3	109,000(485.0)		
5	30.1/1	114,600(509.9)	123,033(547.4)	4350(30.0)
	30.1/2	130,000(578.4)		
	30.1/3	124,500(553.9)		

face of the ribs in two locations (Fig. 6):

(1) At the centre of the joint core

and

(2) Along the edges of the joint core.

Adhesive M-bond AE-10 was used to glue strain gauges to concrete surface. Gauge installation was done according to Vishay Intertechnology specifications.

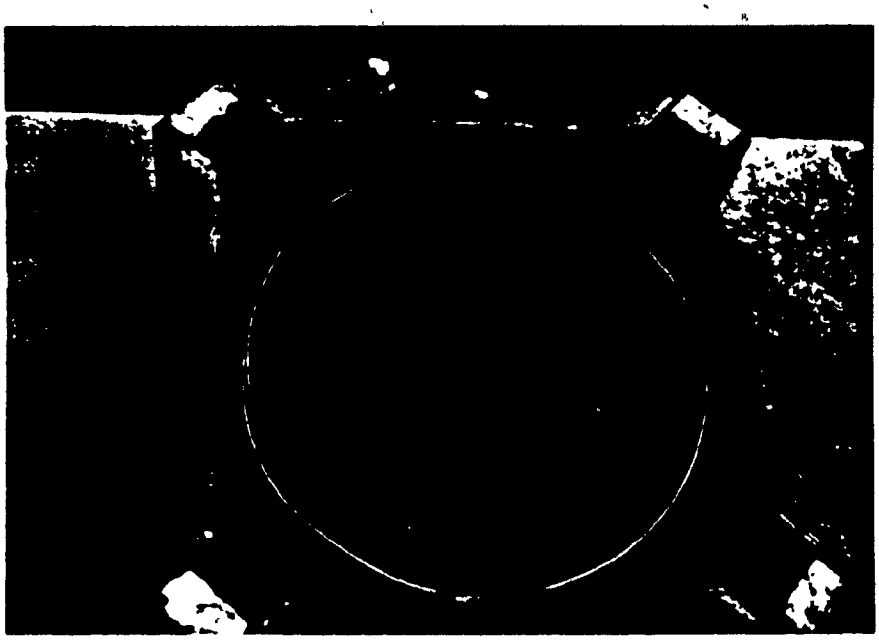

Fig. 5 Specimen formwork with the reinforcing bar in the slab area

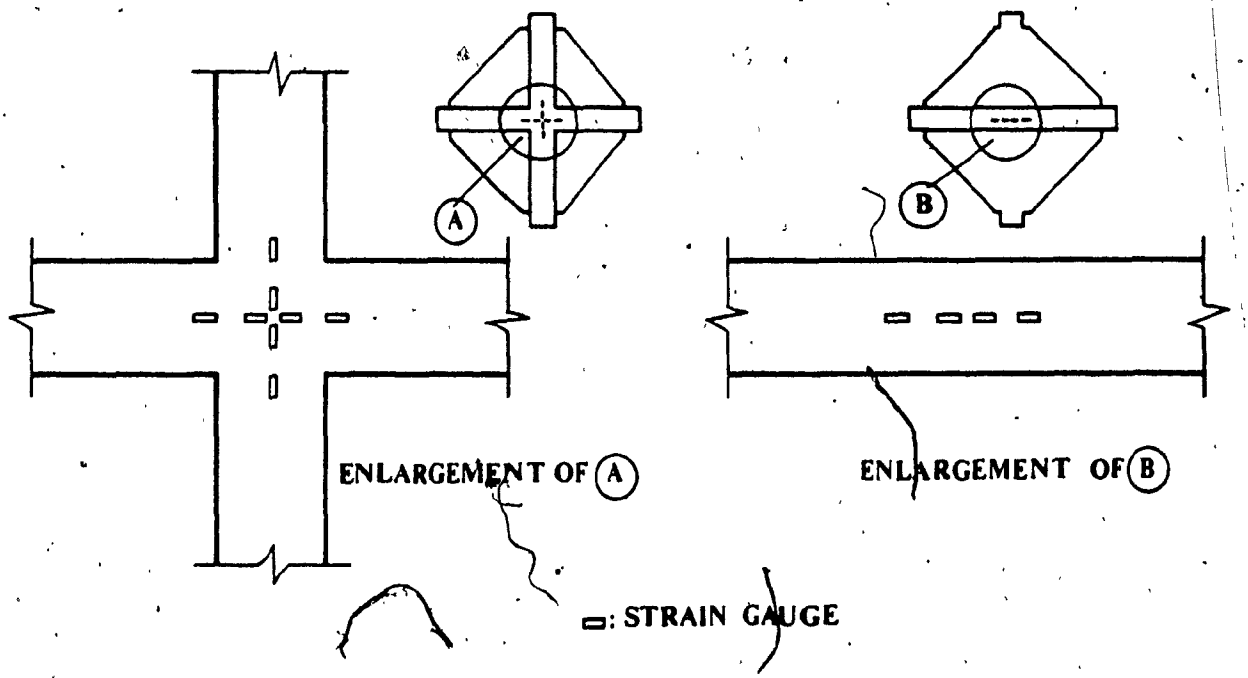

Fig. 6 Positions of strain gauges in one-way and two-way specimen

TESTING PROCEDURE

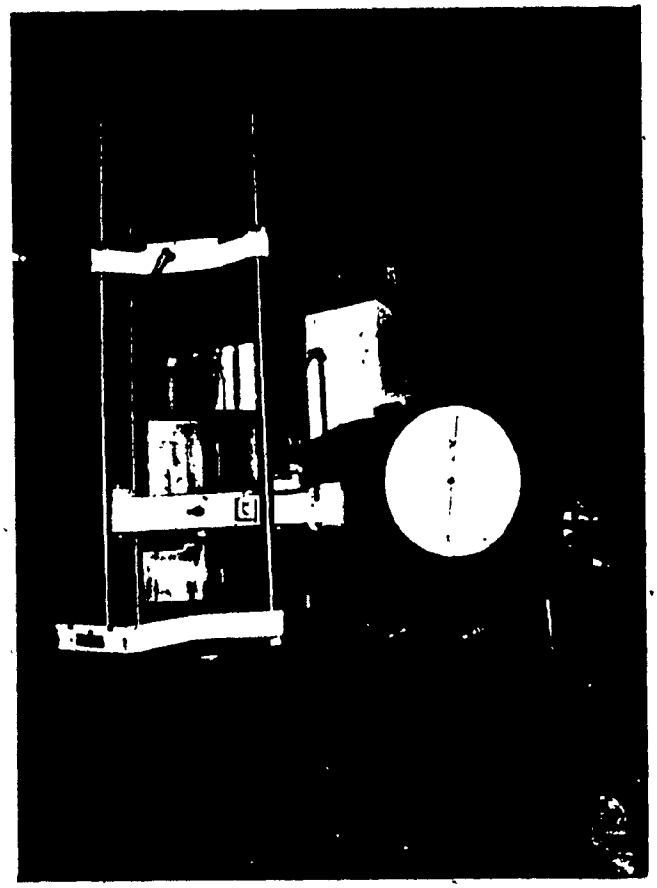

Fig. 7 Overall view of testing machine

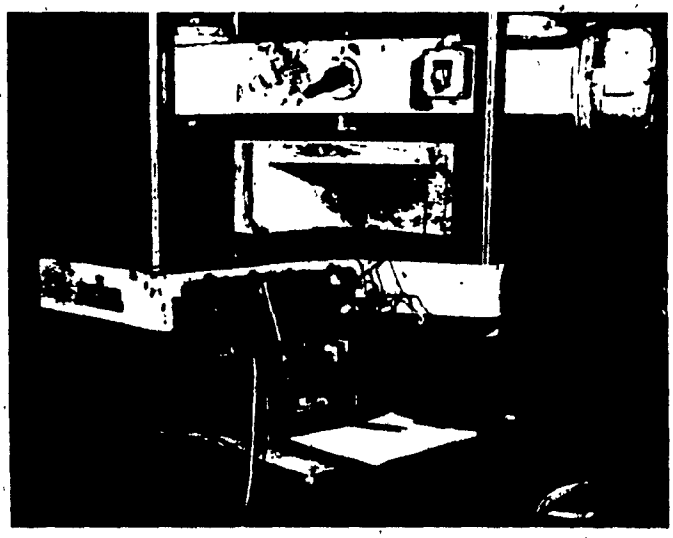

Fig. 8 Strain indicator and specimen on testing machine

Tests were done on a Tinius Olsen testing machine (Fig. 7). The test specimen was placed in the centre of the machine (Fig.8) on rolling supports which consisted of steel bar and steel platen (Fig.9b).

Uniaxial tension stress state was achieved by supporting the specimen at the ends of one rib only (Fig.9), leaving cross rib free or unsupported (in case of two-way ribbed specimens).

Biaxial tension was achieved by supporting the specimen at the ends of each rib (Fig. 10). Attention was given to supports so that each could be activated from the instant the specimen was placed on the machine. In some cases of biaxial loading, shims were called for proper adjust-

ment of specimen on the rollers. In both support conditions, load was applied in the middle of the slab.

During the test, strain deformations were recorded at load increments of 500 lbs (2.2 kn) using the Vishay intertechnology strain indicator seen in Fig. 8.

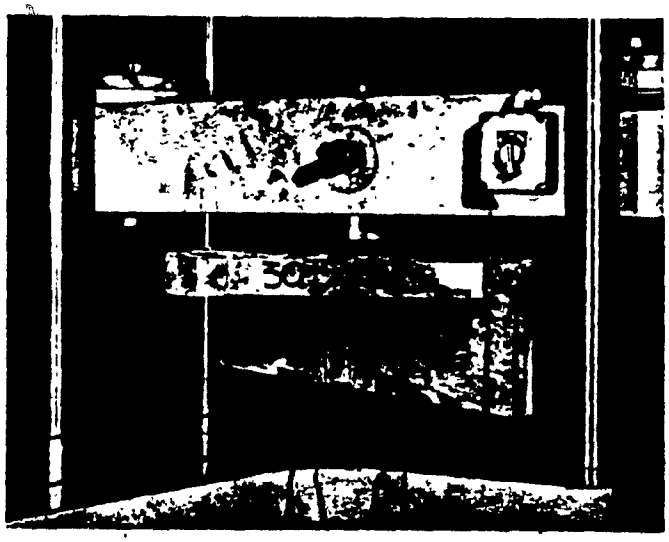

Fig. 9 Support conditions for uniaixial tension tests

(a) One-way ribbed slab specimen

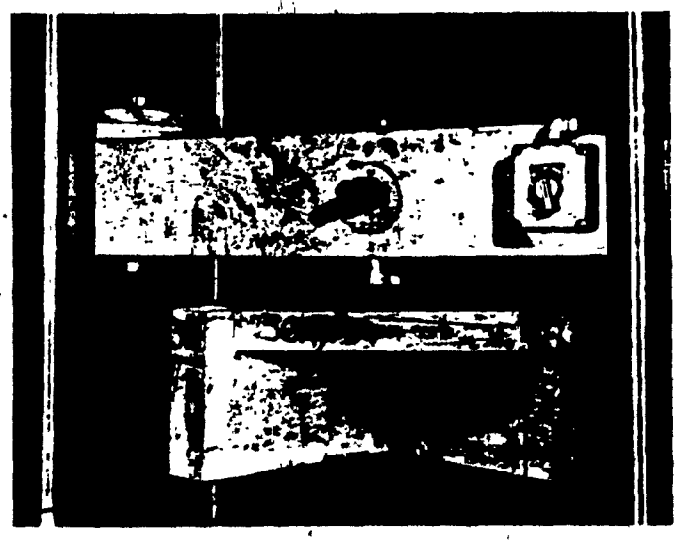

(b) Two-way ribbed slab specimen

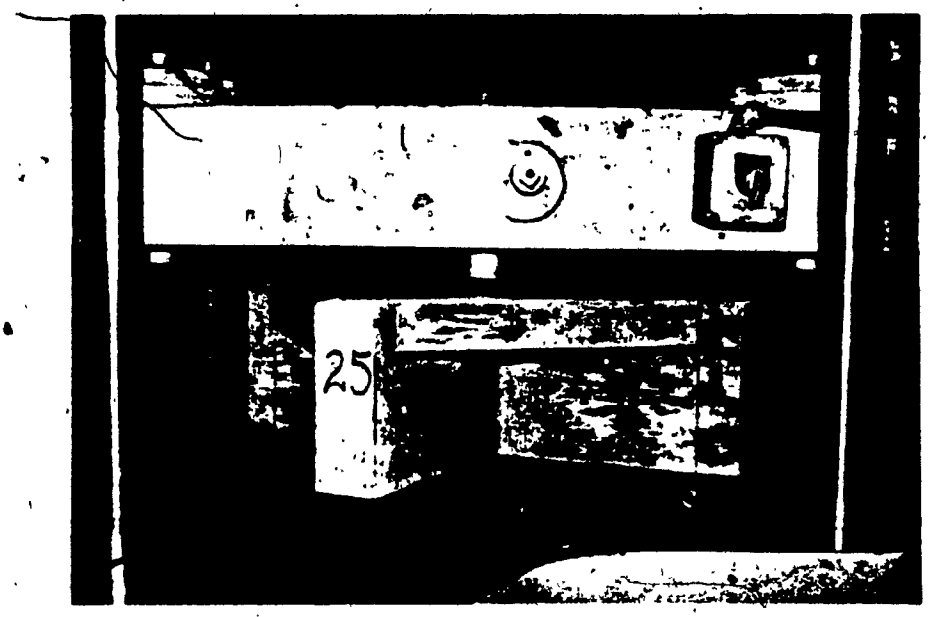

Fig. 10 Support condition for biaxial tension tests

TEST RESULTS

FAILURE MODES

Figures 11 and 12 show crack patterns in the specimens after failure. In most cases, one continuous crack across the specimen perpendicular to the tensile strains was formed in the samples tested under uniaxial tension. No other cracks, apart from the "fatal" crack were observed.

In biaxial tension, behaviour was different. Basically, two types of cracks were observed: a single diagonal crack, having an angle of 45° or so to the principal tensile strains, or a Y-shaped crack starting from the joint core area and branching towards the slab perimeter. Additional microcracks on bottom slab surface and around the supports were observed as well.

In both uniaxial and biaxial tension tests, failure was sudden. At the instant of failure, load commenced decreasing, indicating that the specimen had failed before cracks could be observed.

THE STRAINS

Strains in the principal directions were recorded for all tests. Figures 13 through 19 show the variation of strain ε versus P/f_c' where P stands for the applied concentrated load and f_c' for the compressive strength of concrete, established on standard 6 in (15 cm) diameter cylinders.

Figure 13 shows comparison of tensile strain in the uniaxial (one-way ribbed specimens) and biaxial (two-way ribbed specimens) stress states. Tensile strain ε_b^+ in biaxial loading is approximately one-third of the tensile strain ε_u^t in uniaxial loading, with maximum

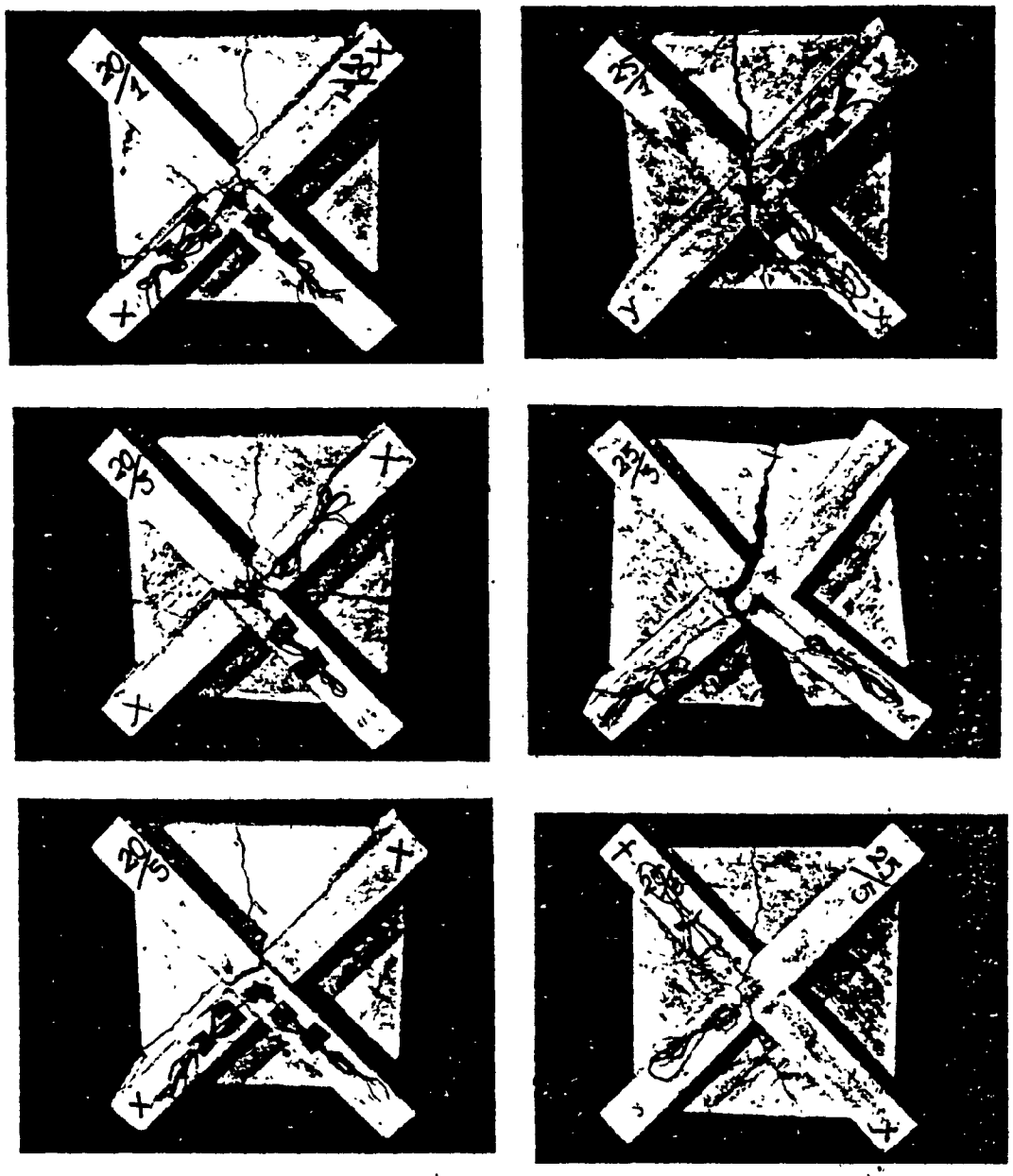

Fig. 11a. Failure Modes of Specimens Tested Under Biaxial Loading, Seen from the Bottom side (Series No. 1 and No. 2)

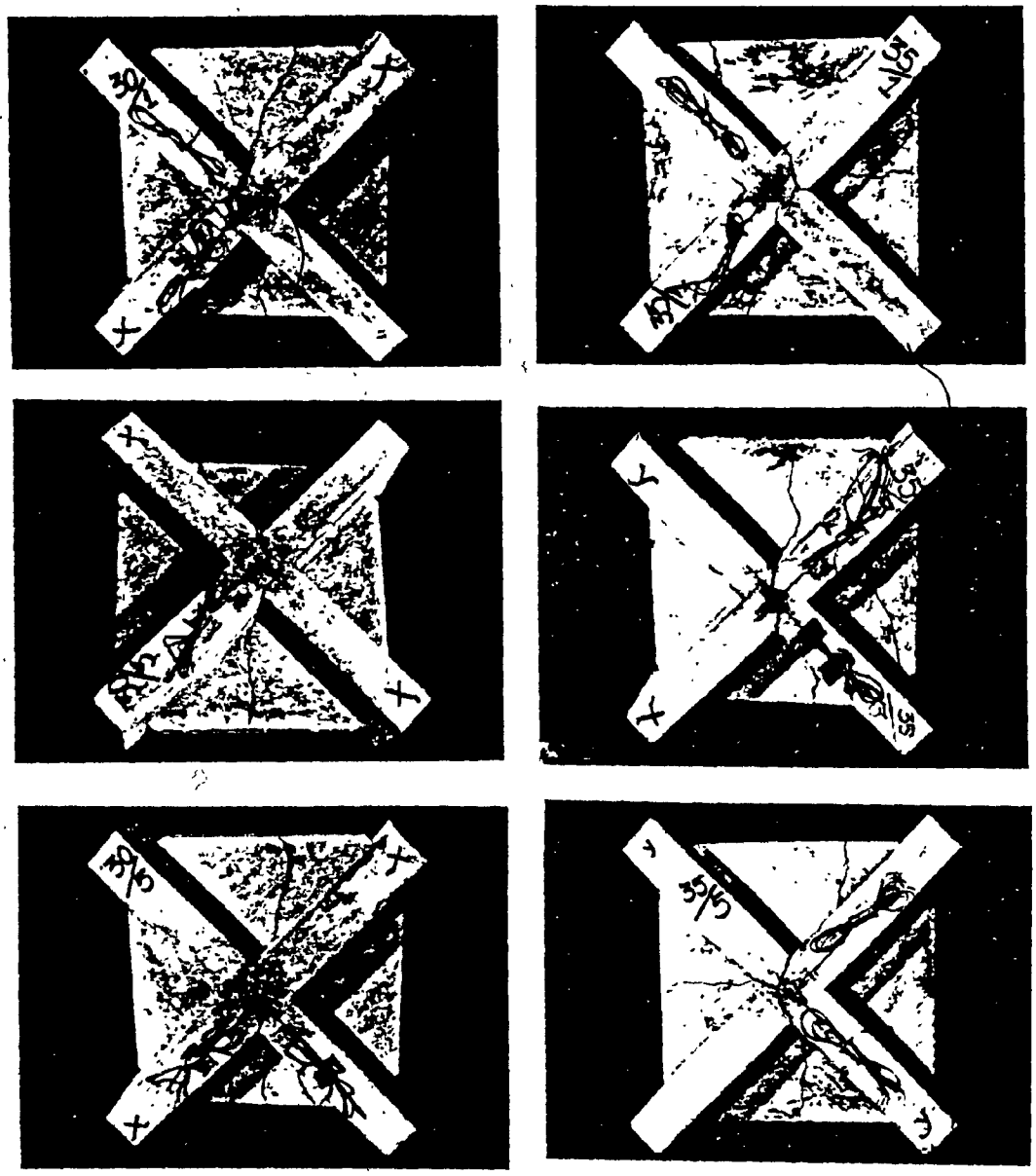

Fig. 11b. Failure Modes of Specimens Tested Under Biaxial Loading, Seen From the Bottom Side (Series No. 3 and No. 4)

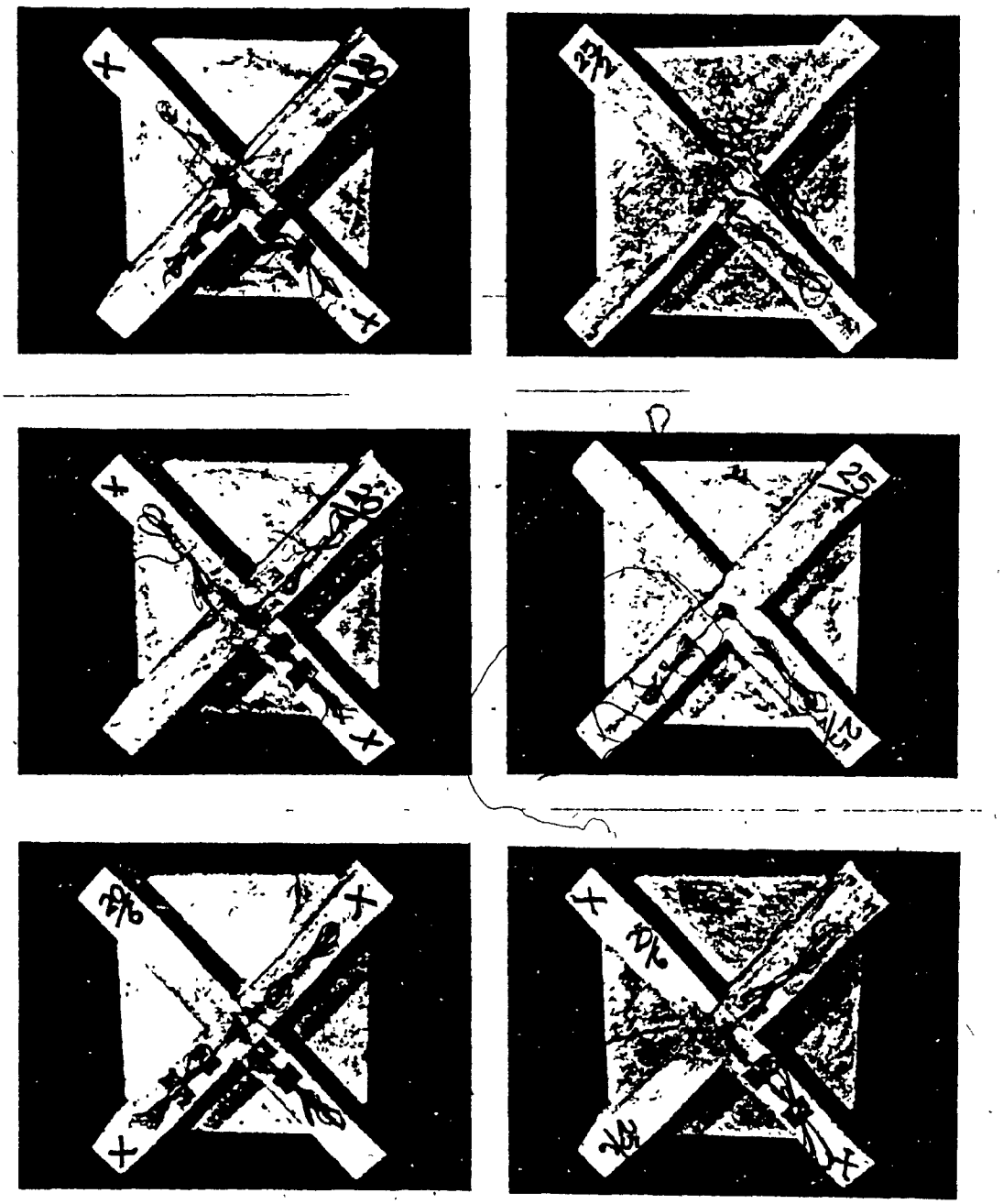

Fig. 12a. Failure Modes of Specimens Tested Under Uniaxial Loading, Seen from the Bottom Side (Series No. 1 and No. 2)

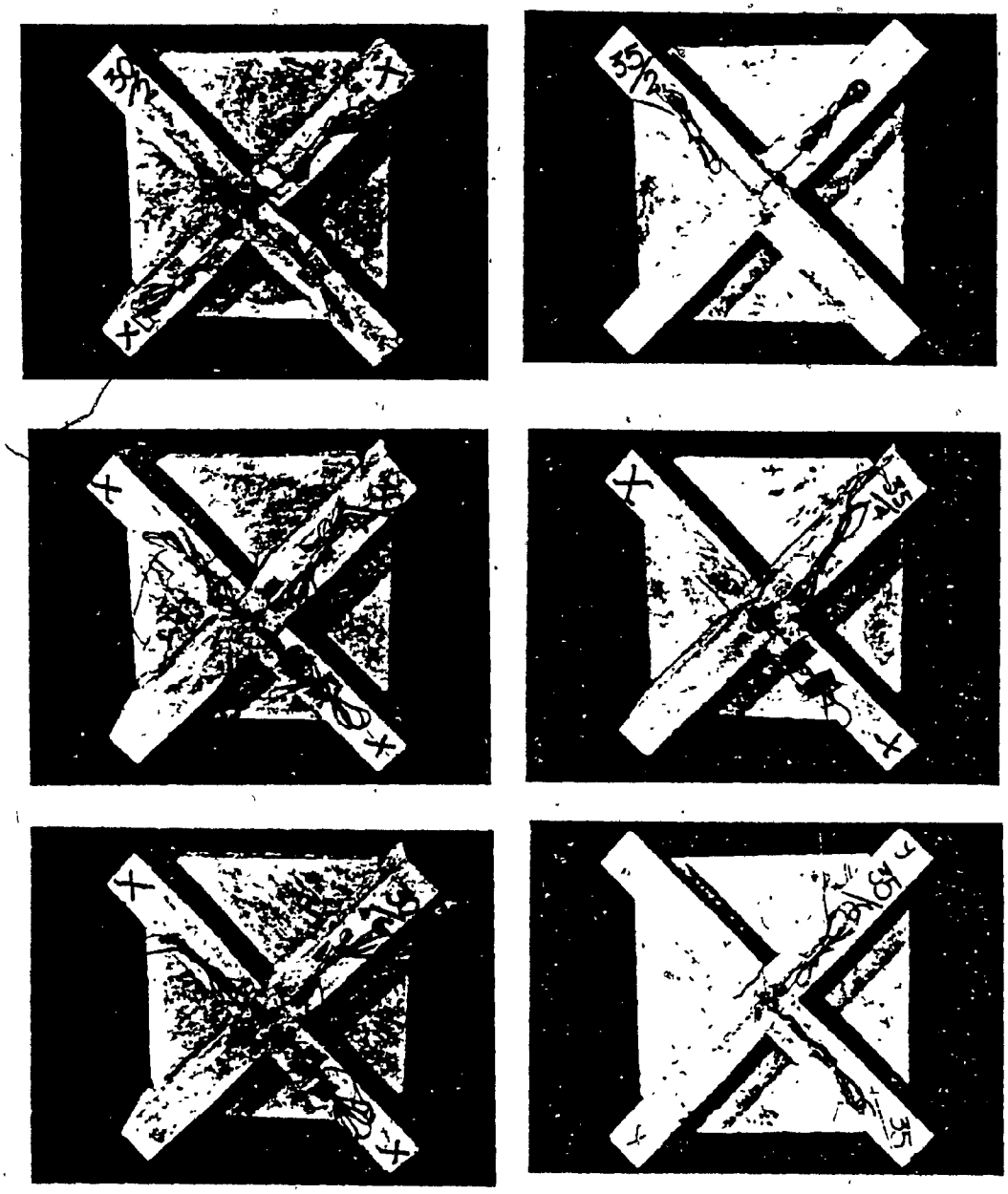

Fig. 12b. Failure Modes of Specimens Tested Under Uniaxial Loading, Seen from the Bottom Side (Series No. 3 and No. 4)

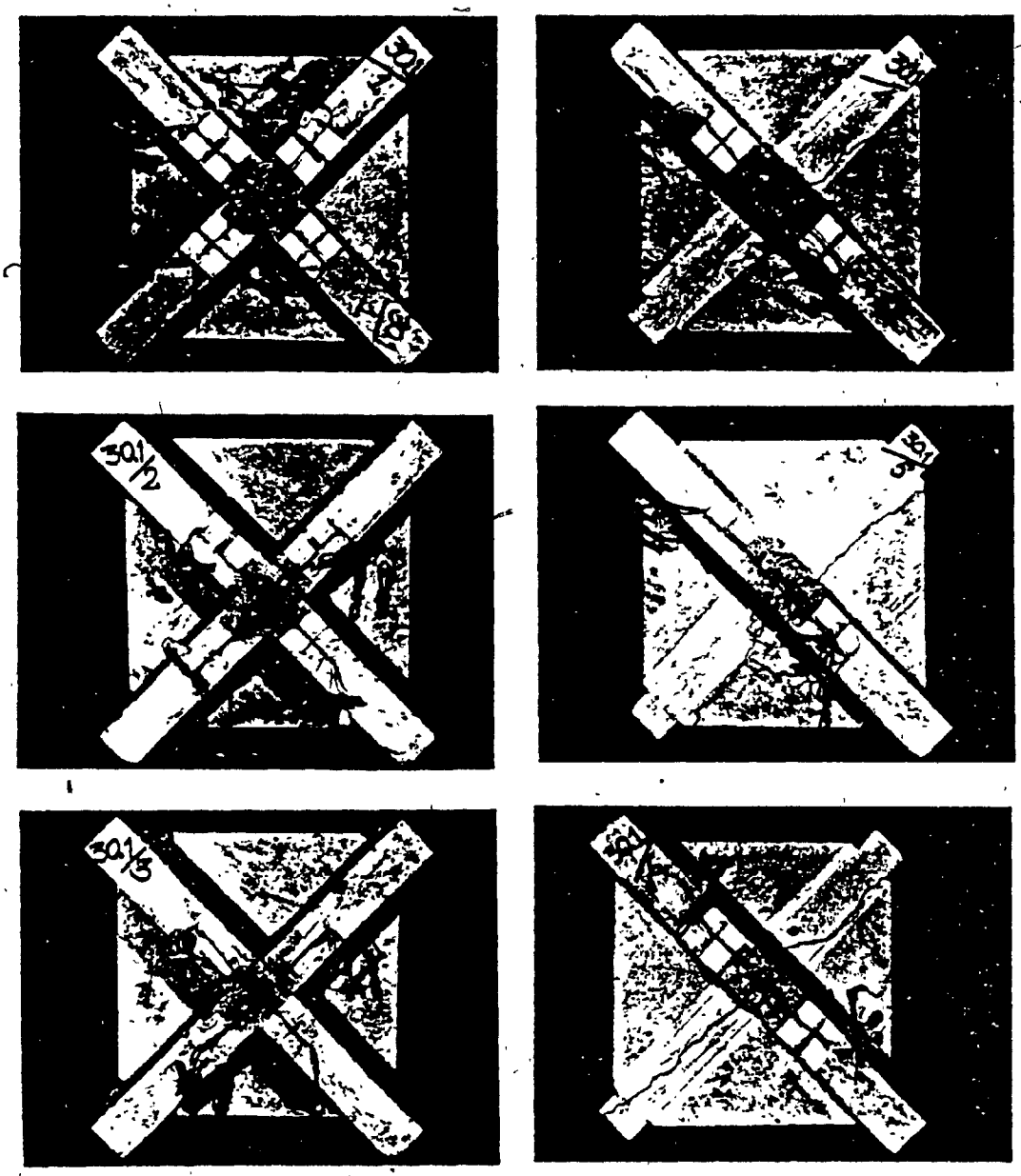

Fig. 12c. Failure Modes of Specimens Tested Under Uniaxial Loading, Seen from the Bottom Side (Series No. 5)

DATA FOR CURVE A						
SERIES 30.1						
f'_c (psi)	P (lbs)	P/f'_c	STRAIN(μin/in) SPECIMEN 30.1/4	30.1/5	30.1/6	AVERAGE STRAIN (μin/in)
	375	0.09	10		16	(13)
	875	0.20	19		42	(30.5)
	1375	0.32	27	39.5	60.5	42.3
	1875	0.43	35.5	53	83.5	57.3
	2375	0.55	44.5	64	103	70.5
	2875	0.66	51	78	128.5	85.8
4350	3375	0.78	59	88.5	152.5	100
	3875	0.89	63.5	99	182	114.8
	4375	1.01	68	109.5	209	128.8
	4875	1.12	70	118.5	249	145.8
	5375	1.24	75	127.5	290	164.2
	5875	1.35			560	

TABLE 2a Strain measurements plotted in Fig. 13

DATA FOR CURVE B							
f'_c (psi)	P (lbs)	P/f'_c	STRAIN(μin/in) SERIES 20	25	30	35	AVERAGE STRAIN (μin/in)
	350	0.09	4.5	(4.5)	2.3	6	4.3
	850	0.23	9.5	(9.5)	6.5	8.7	8.6
	1350	0.36	17.3	12.7	10	12.7	13.2
	1850	0.49	22.5	18	13.2	17.5	17.8
	2350	0.63	29.5	23.5	16.2	22.	22.8
	2850	0.76	36.2	28.3	19.8	26.8	27.8
3750	3350	0.89	42.8	34.5	23.8	32.2	33.3
	3850	1.03	48.3	40.3	27.5	36	38
	4350	1.16	55.2	44.3	31.2	41.5	43.1
	4850	1.29	60.8	47.7	35.7	47.2	47.9
	5350	1.43	67.3	46.8	42.7	52.7	52.4
	5850	1.56	73.3	36.7	50.5	57.3	54.5
	6350	1.69	79.2		62.5	62.5	(68.1)
	6850	1.83	82.2			66.7	(74.5)
	7350	1.96				68.8	
	7850	2.09				71.7	

TABLE 2b Strain measurements plotted in Fig. 13

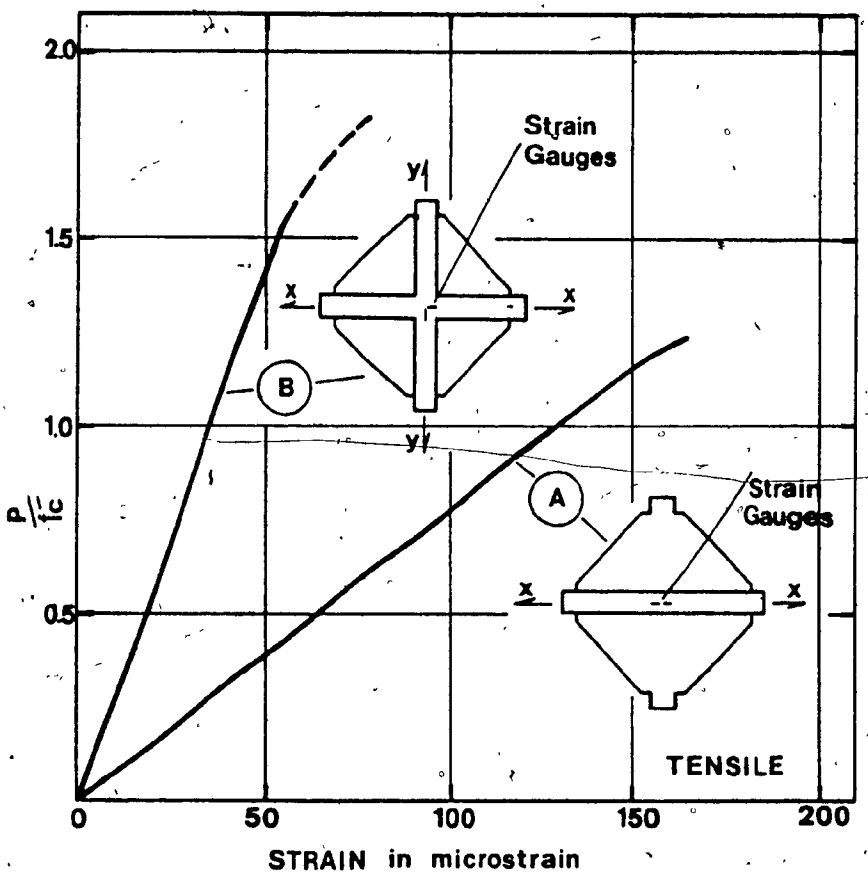

CURVE (A) IS THE AVERAGE OF 3 TESTS
CURVE (B) IS THE AVERAGE OF 12 TESTS

Fig. 13 Comparison of tensile strains in one-way ribbed specimens under uniaxial loading (Curve A) and in two-way ribbed specimens under biaxial loading (Curve B). Strain gauges are attached to the centre of the bottom face.

values about +80 and +165 microstrain respectively. Both strain variations are almost linear up to failure.

Figure 14 shows an average uniaxial tensile strain in one-way and two-way ribbed specimens. Tensile strains change almost equally, with maximum values about +165 and +200 microstrain in one-way and two-way specimens respectively.

Figure 15 shows an average variation of tensile and compressive strains* in two-way specimens tested uniaxially. Compressive strain* is nearly one-third of tensile strain all the way up to failure. Maximum value of tensile and compressive strain is about + 200 and |-60| microstrain respectively.

Figures 16 through 19 show the strain variation in each series individually under uniaxial and biaxial loading.

* compressive strain = strain due to contraction in the free or unsupported rib

DATA FOR CURVE A								
f'_c (psi)	P (lbs)	P/f'_c	TENSILE STRAIN(μin/in) SERIES					AVERAGE STRAIN (μin/in)
			20	25	30	35	30.1	
	350	0.09	13.7	17.3	16.7		12.7	(15.1)
	350	0.22	32.7	34	30.7	30	29.2	31.3
	1350	0.35	49.7	53.7	48.7	48.7	45.5	49.3
	1850	0.48	69.7	68	68.3	68.7	61.7	67.3
	2350	0.61	86	84.7	86.3	88.7	76.7	84.5
3870	2850	0.74	108	106.7	112.7	113.7	84.3	105.1
	3350	0.87	127.7	140.3	138.7	140.7	93.8	128.2
	3850	1.00		162	179.3	172.7	102.8	(154.2)
	4350	1.12		192.7	237.3	274.7	108.7	(203.4)
	4850	1.25				311.7	87.2	

TABLE 3a Strain measurements plotted in Fig. 14a.

DATA FOR CURVE B						
SERIES 30.1						
f'_c (psi)	P (lbs)	P/f'_c	STRAIN(μin/in) SPECIMEN			AVERAGE STRAIN (μin/in)
			30.1/4	30.1/5	30.1/6	
	375	0.09	10		16	(13)
	875	0.20	19		42	(30.5)
	1375	0.32	27	39.5	60.5	42.3
	1875	0.43	35.5	53	83.5	57.3
	2375	0.55	44.5	64	103	70.5
	2875	0.66	51	78	128.5	85.8
4350	3375	0.78	59	88.5	152.5	100
	3875	0.89	63.5	99	182	114.8
	4375	1.01	68	109.5	209	128.8
	4875	1.12	70	118.5	249	145.8
	5375	1.24	75	127.5	290	164.2
	5875	1.35			560	

TABLE 3b Strain measurements plotted in Fig. 14a.

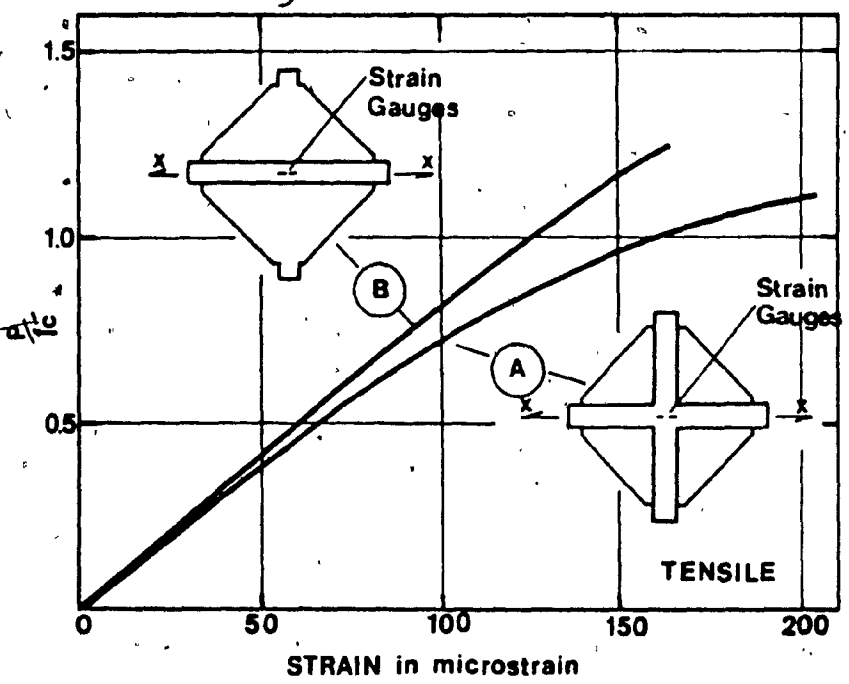

Fig. 14a Comparison of tensile strains in two-way ribbed specimens (Curve A) and in one-way ribbed specimens (Curve B), both loaded uniaxially. Strain gauges are attached to the centre of the bottom face.

DATA FOR CURVE A						
f'_c (psi)	P (lbs)	P/f'_c	STRAIN(μin/in) SERIES 20	30	30.1	AVERAGE STRAIN (μin/in)
	350	0.09	14	13.3	13.2	13.5
	850	0.22	29.3	25.7	26.8	27.3
	1350	0.35	47.7	38.7	40	42.1
3833	1850	0.48	63	54	53.2	56.7
	2350	0.61	78.7	65.3	66.8	70.3
	2850	0.74	92.7	79.7	81	84.5
	3350	0.87	105.7	92.3	94.8	97.6
	3850	1.00	(129)	106	106.3	113.8
	4350	1.13	(149.5)	123	104.1	125.7
	4850	1.27		124	98.3	
	5350	1.40		(172)		
	5850	1.53		(183)		

TABLE 4a Strain measurements plotted in Fig. 14b

DATA FOR CURVE B						
SERIES 30.1						
f'_c (psi)	P (lbs)	P/f'_c	STRAIN(μin/in) SPECIMEN 30.1/4	30.1/5	30.1/6	AVERAGE STRAIN (μin/in)
	375	0.09	11.5		12.5	(12)
	875	0.20	22.5		27.5	(25)
	1375	0.32	38	35	42.5	38.5
	1875	0.43	49	47	54.5	50.2
	2375	0.55	63.5	58	67.5	63
4350	2875	0.66	74.5	68.5	82.5	75.2
	3375	0.78	88	78	98.5	88.2
	3875	0.89	97	77	112	95.3
	4375	1.01	108	79	129	105.3
	4875	1.12	113	84	146	114.3
	5375	1.24	126	75	160.5	120.5
	5875	1.35			171	

TABLE 4b Strain measurements plotted in Fig. 14b

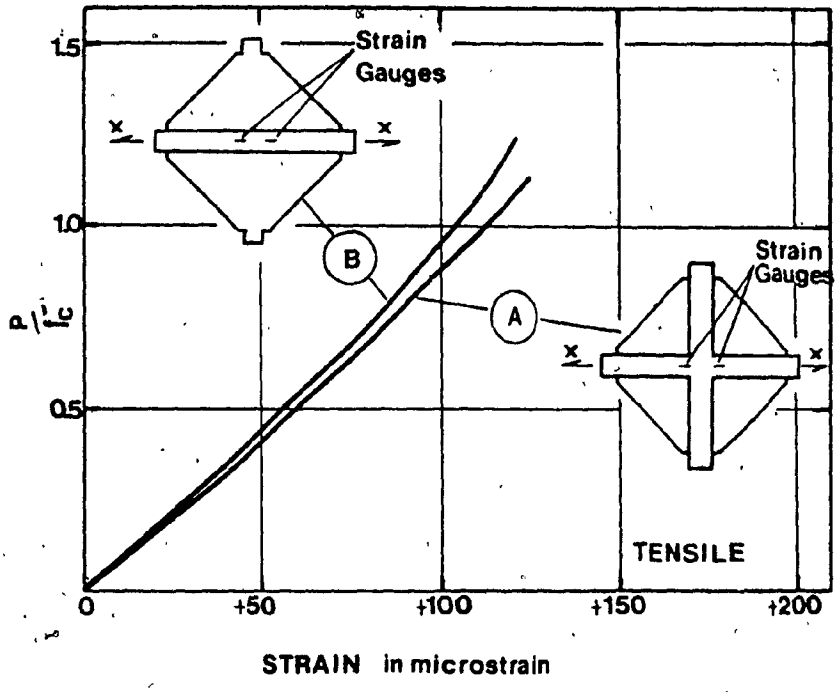

Fig. 14b Comparison of tensile strains in two-way ribbed specimens (Curve A) and in one-way ribbed specimens (Curve B), both loaded uniaxially. Strain gauges are attached along the edges of the joint core.

DATA FOR CURVES A AND B														
f'_c (psi)	P (lbs)	P/f'_c	STRAIN (μin/in) SERIES 20		25		30		35		30.1		AVERAGE STRAIN (μin/in)	
	350	0.09	13.7	- 6.3	17.3	-7	16.7	-7			12.7	-6.5	(15.1)	(-6.7)
	850	0.22	32.7	-14	34	-14	30.7	-13.7	30	-15.7	29.2	-13.8	31.3	-14.2
	1350	0.35	49.7	-22	53.7	-19.3	48.7	-19.3	48.7	-22.3	45.5	-20.5	49.3	-20.7
	1850	0.48	69.7	-30	68	-26	68.3	-26	68.7	-30.3	61.7	-26.8	67.3	-27.8
3870	2350	0.61	86	-37	84.7	-32	86.3	-31	88.7	-36.3	76.7	-33.7	84.5	-34
	2850	0.74	108	-44.7	106.7	-37.7	112.7	-38	113.7	-43.3	84.3	-40.8	105.1	-40.9
	3350	0.87	127.7	-53.3	140.3	-43	138.7	-43.7	140.7	-50	93.8	-47.7	128.2	-47.5
	3850	1.00			162	-47.3	179.3	-50	172.7	-54.7	102.8	-53.7	(154.2)	(-51.4)
	4350	1.12			192.7	-49.7	237.3	-51.3	274.7	-61.3	108.7	-59.5	(203.4)	(-55.5)
	4850	1.25						-55.7	311.7	-69	87.2	-65.2		

TABLE 5 (Average) strain measurements plotted in Fig. 15

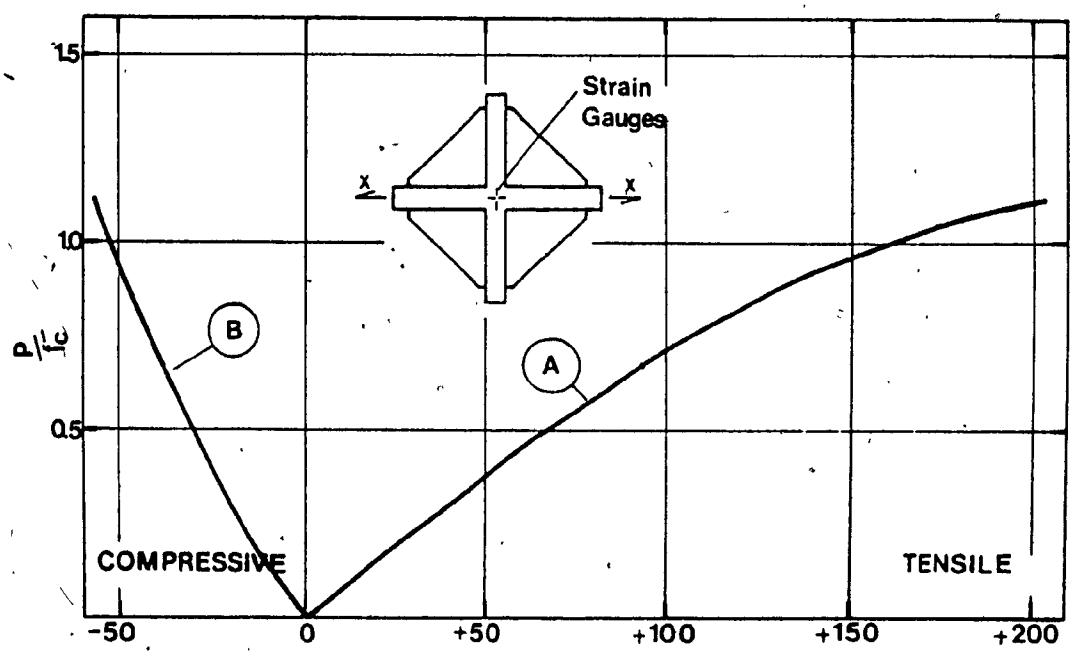

Fig. 15 Tensile and compressive strain* variation in two-way ribbed specimens uniaxially loaded. Strain gauges are attached to the centre of the bottom face.

* compressive strain = strain due to contraction in the free or unsupported rib

SERIES 20						
f'_c (psi)	P (lbs)	P/f'_c	STRAIN(μin/in) SPECIMEN 20/1	20/3	20/5	AVERAGE STRAIN (μin/in)
	350	0.10	3	6.5	4	4.5
	850	0.25	6	12	10.5	9.5
	1350	0.39	13	18	21	17.3
	1850	0.54	17	24.5	26	22.5
	2350	0.69	21	32	35.5	29.5
	2850	0.83	26	38.5	44	36.2
	3350	0.98	31.5	46	51	42.8
	3850	1.12	35.5	52.5	57	48.3
	4350	1.27	41	60	64.5	55.2
	4850	1.41	46.5	67	69	60.8
3430	5350	1.56	51	75	76	67.3
	5850	1.71	56	82.5	81.5	73.3
	6350	1.85	61	90.5	86	79.2
	6850	2.00	58	98.5	90	82.2
	7350	2.14		107	94.5	
	7850	2.29		114	96.5	
	8350	2.43		123.5	105	
	8850	2.58		132		
	9350	2.73		146		
	9850	2.87		158		
	10350	3.01		164		

TABLE 6 Strain measurements plotted in Fig. 16a

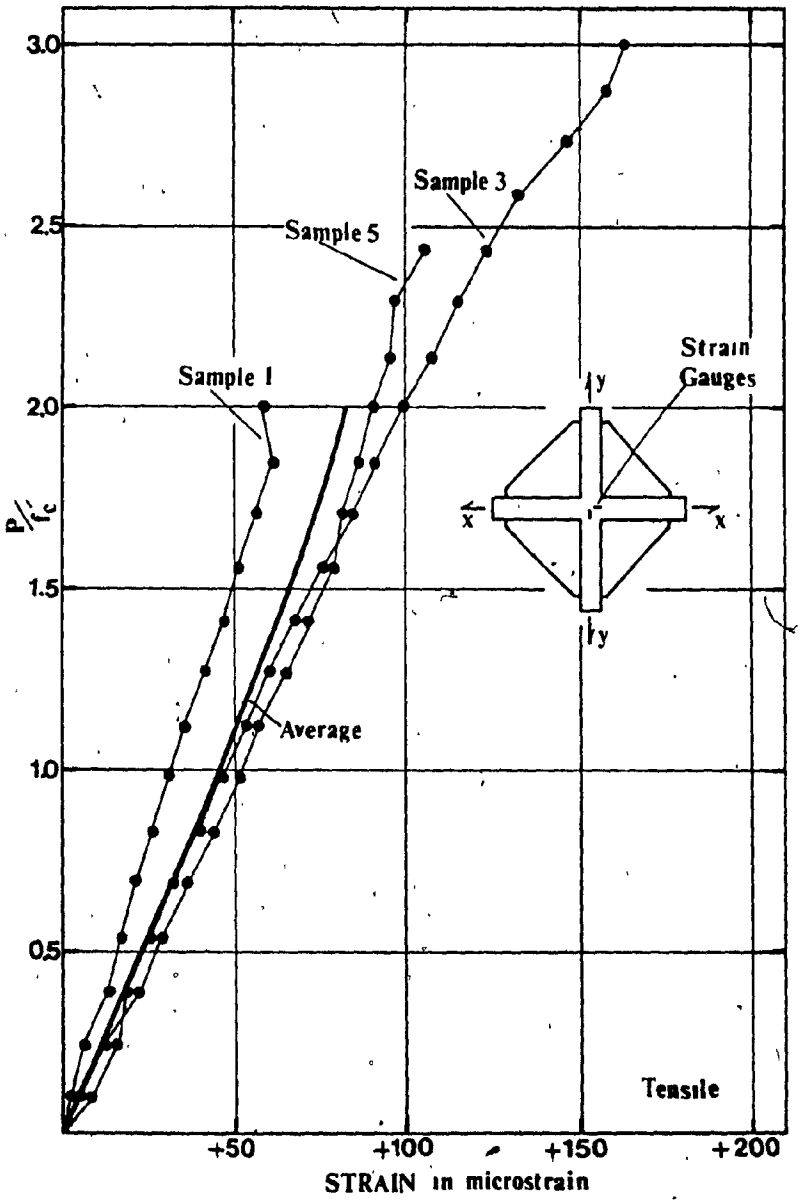

Fig. 16a Tensile strain variation in two-way ribbed specimens biaxially loaded of Series 20. Strain gauges are attached to the centre of the bottom face.

SERIES 25						
f'_c (psi)	P (lbs)	P/f'_c	STRAIN (μin/in) SPECIMEN 25/1	25/3	25/5	AVERAGE STRAIN (μin/in)
3830	350	0.09	4		5	(4.5)
	850	0.22	9.5		9.5	9.5
	1350	0.35	14	10	14	12.7
	1850	0.48	19	15.5	19.5	18
	2350	0.61	24.5	20	26	23.5
	2850	0.74	30	24	31	28.3
	3350	0.87	35.5	30	38	34.5
	3850	1.00	39	34.5	47.5	40.3
	4350	1.14	44	41	48	44.3
	4850	1.27	48	48	47	47.7
	5350	1.40	51.5	50	39	46.8
	5850	1.53	57	53	0	36.7
	6350	1.66	58		-40	
	6850	1.79	53			
	7350	1.92	37			
	7850	2.05	47.5			
	8350	2.18	31.5			

TABLE 7 Strain measurements plotted in Fig. 16b

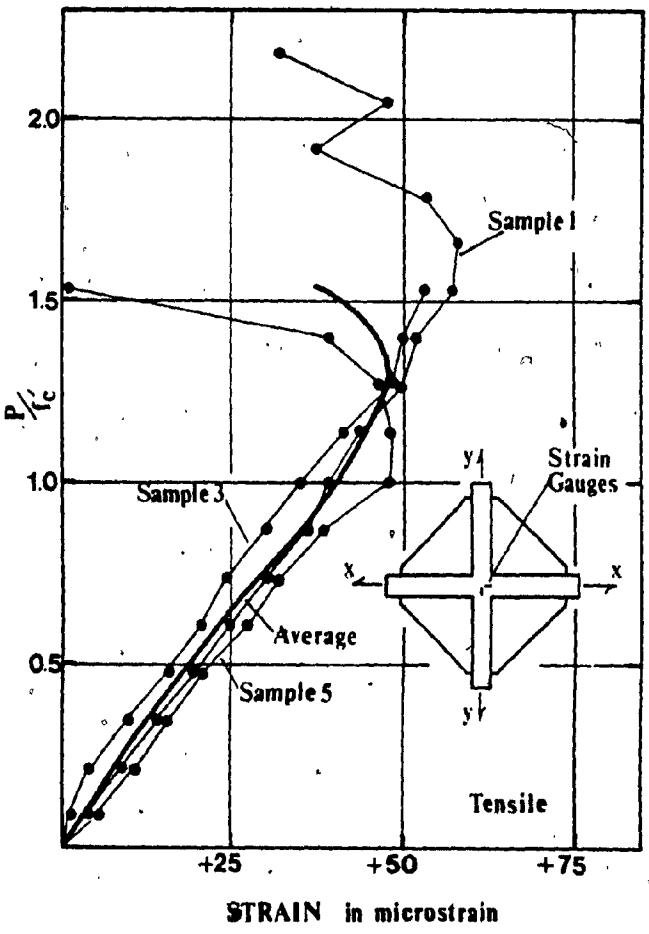

Fig. 16b Tensile strain variation in two-way ribbed specimens biaxially loaded of Series 25. Strain gauges are attached to the centre of the bottom face.

SERIES 30						
f'_c (psi)	P (lbs)	P/f'_c	STRAIN (μin/in) SPECIMEN 30/1	30/3	30/5	AVERAGE STRAIN (μin/in)
	350	0.09	1	3.5	2.5	2.3
	850	0.23	4.5	8.5	(-1.5)	6.5
	1350	0.36	7.5	16	6.5	10
	1850	0.50	10	20	9.5	13.2
	2350	0.63	12	25	11.5	16.2
	2850	0.77	15.5	29	15	19.8
	3350	0.9	19	34	18.5	23.8
	3850	1.03	22	38.5	22	27.5
3720	4350	1.17	24.5	43.5	25.5	31.2
	4850	1.30	27.5	48.5	31	35.7
	5350	1.44	36	51.5	40.5	42.7
	5850	1.57	41	55.5	55	50.5
	6350	1.71	50.5	60	77	62.2
	6850	1.84	57	65		
	7350	1.98	67	71.5		
	7850	2.11	75.5	76		
	8350	2.24	79.5	80		
	8850	2.38		84		
	9350	2.51		82.5		

TABLE 8 Strain measurements plotted in Fig. 16c

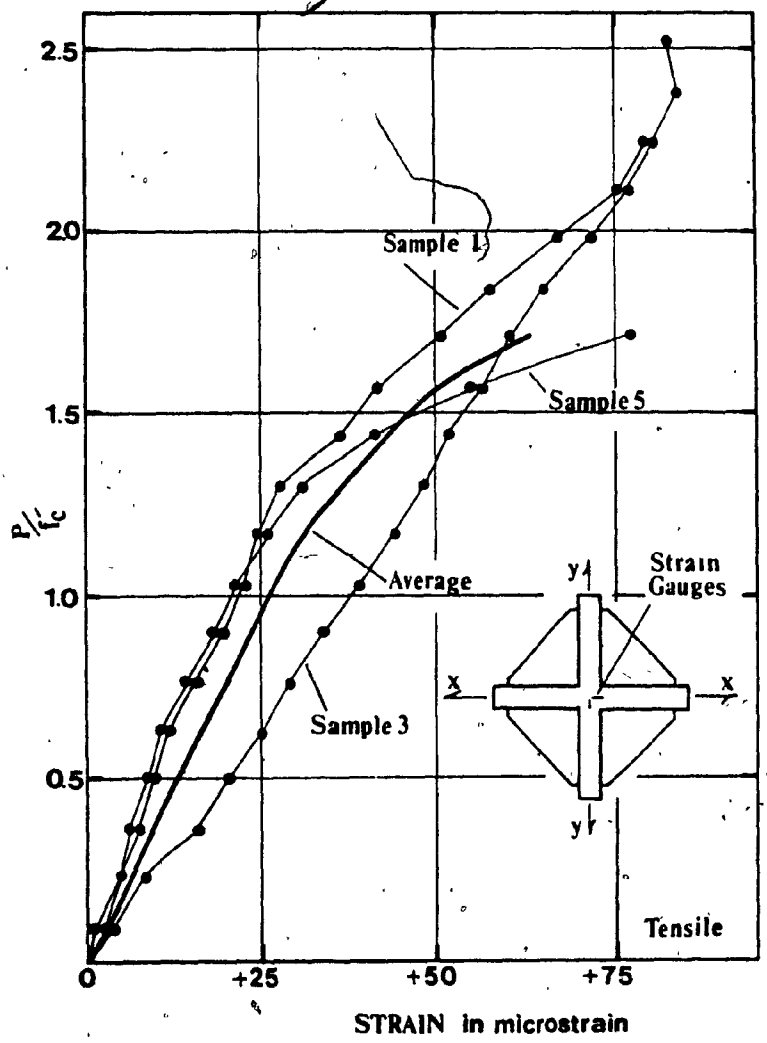

Fig. 16 c Tensile strain variation in two-way ribbed specimens biaxially loaded of Series 30. Strain gauges are attached to the centre of the bottom face.

SERIES 35						
f'_c (psi)	P (lbs)	P/f'_c	STRAIN (μin/in) SPECIMEN			AVERAGE STRAIN (μin/in)
			35/1	35/3	35/5	
	350	0.09	3	5	4	6
	850	0.21	5.5	9.5	11	8.7
	1350	0.34	9	12	17	12.7
	1850	0.46	11.5	17	24	17.5
	2350	0.58	15	21	30	22
	2850	0.71	19	25.5	36	26.8
	3350	0.83	22.5	31	43	32.2
	3850	0.96	25	35	48	36
4020	4350	1.08	27.5	41.5	55.5	41.5
	4850	1.21	32	46.5	63	47.2
	5350	1.33	35.5	52	70.5	52.7
	5850	1.46	39	58	75	57.3
	6350	1.58	42.5	64	81	62.5
	6850	1.70	44	72.5	83.5	66.7
	7350	1.83	37	80	89.5	68.8
	7850	1.95	60.5	86.5	68	71.7
	8350	2.08	58.5	94.5		
	8850	2.2	62	101		
	9350	2.33		58		

TABLE 9 Strain measurements plotted in Fig. 16d

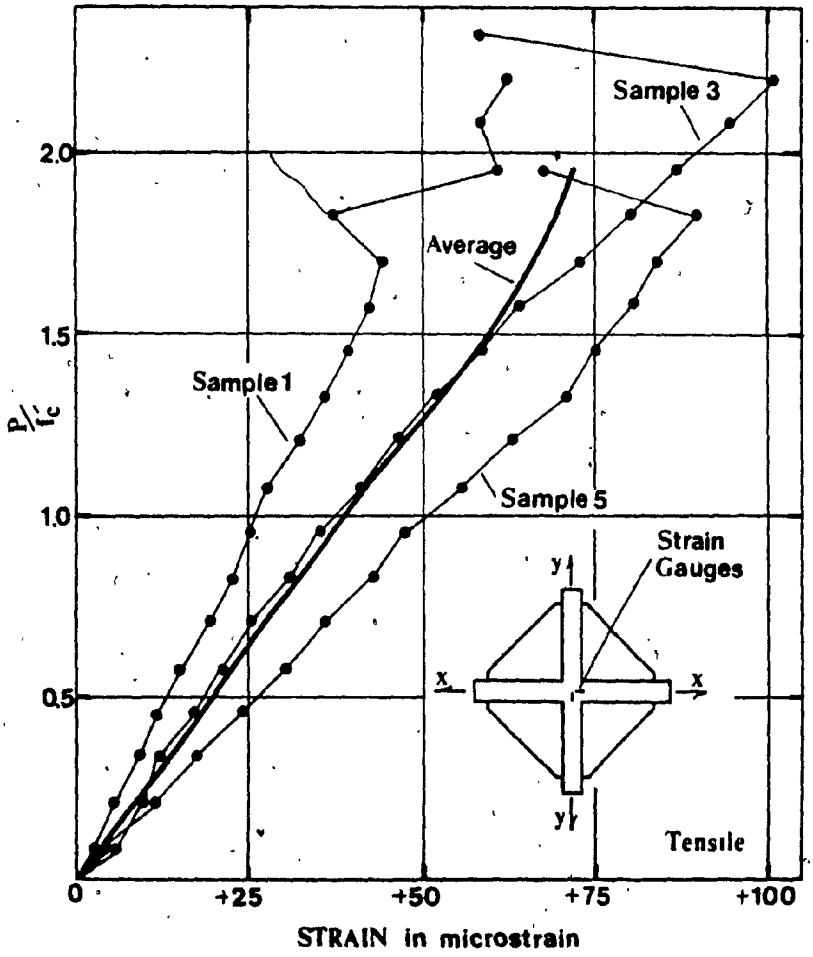

Fig. 16d Tensile strain variation in two-way ribbed specimens biaxially loaded of Series 35. Strain gauges are attached to the centre of the bottom face.

SERIES 20										
f'_c (psi)	P (lbs)	P/f'_c	STRAIN(μin/in) SPECIMEN 20/2		20/4		20/6		AVERAGE STRAIN (μin/in)	
	350	0.10	14	-8	14	-4	13	-7	13.7	-6.3
	850	0.25	30	-15	38	-11	30	-16	32.7	-14
	1350	0.39	46	-23	57	-18	46	-25	49.7	-22
	1850	0.54	64	-32	82	-25	63	-33	69.7	-30
3430	2350	0.69	78	-39	102	-30	78	-42	86	-37
	2850	0.83	95	-46	133	-38	96	-50	108	-44.7
	3350	0.98	113	-54	160	-46	110	-60	127.7	-53.3
	3850	1.12	124	-62			126	-69		
	4350	1.27	135	-68			136	-73		

TABLE 10 Strain measurements plotted in Fig. 17a

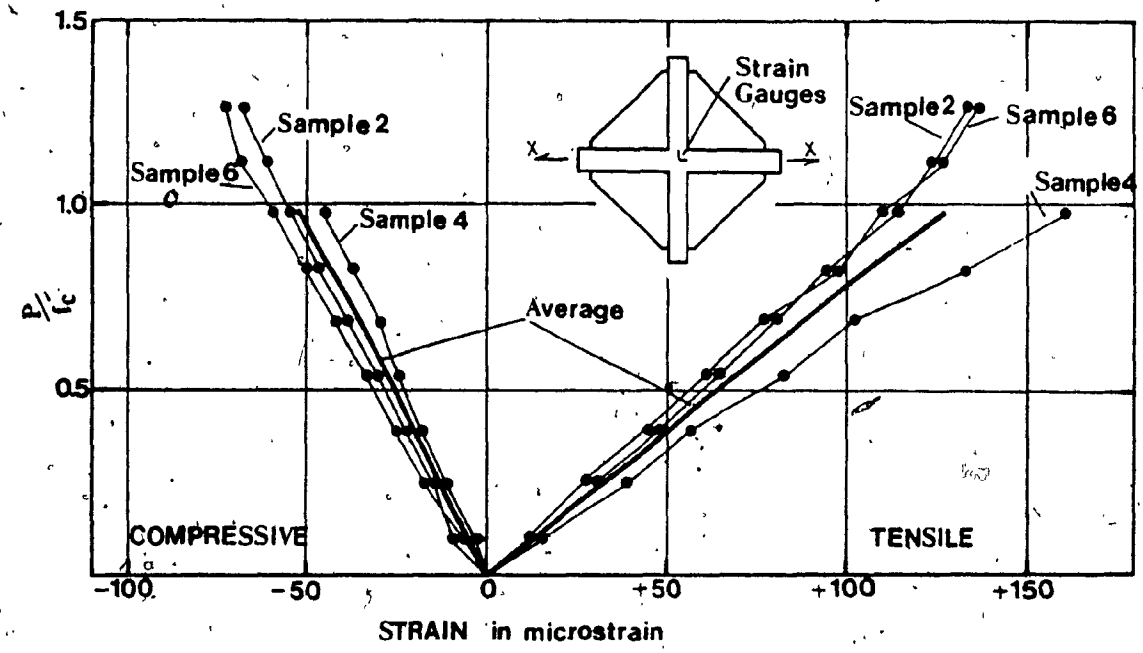

Fig. 17a Tensile and compressive strain* variation in two-way ribbed specimens uniaxially loaded of Series 20. Strain gauges are attached to the centre of the bottom face.

*compressive strain = strain due to contraction in the free or unsupported rib (same in fig. 17b through 17e)

SERIES 25										
f'_c (psi)	P (lbs)	P/f'_c	STRAIN (μin/in) SPECIMEN 25/2		25/4		25/6		AVERAGE STRAIN (μin/in)	
	350	0.09	14	-5	20	-8	18	-8	17.3	-7
	850	0.22	32	-12	38	-15	32	-15	34	-14
	1350	0.35	53	-18	52	-20	56	-20	53.7	-19.3
	1850	0.48	74	-24	69	-26	61	-28	68	-26
3830	2350	0.61	98	-30	80	-32	76	-34	84.7	-32
	2850	0.74	134	-34	94	-39	92	-40	106.7	-37.7
	3350	0.87	212	-40	104	-45	105	-44	140.3	-43
	3850	1.00	258	-42	108	-50	120	-50	162	-47.3
	4350	1.14	340	-43	108	-52	130	-54	192.7	-49.7
	4850	1.27					134	-56		
	5350	1.40					144	-53		

TABLE 11 Strain measurements plotted in Fig. 17b

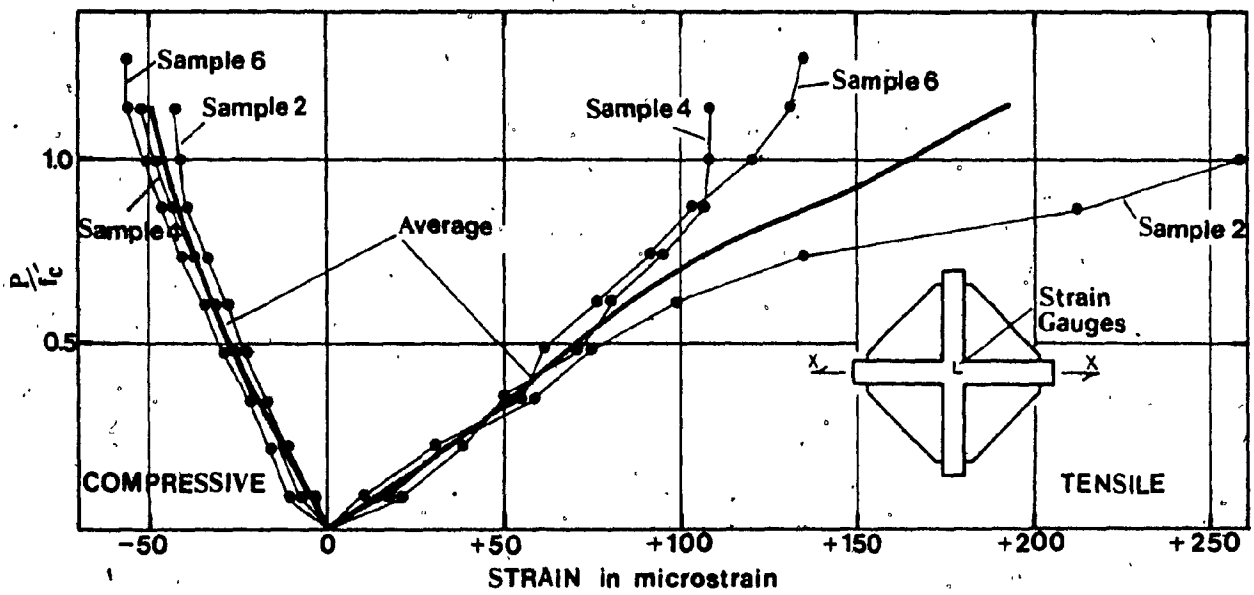

Fig. 17b Tensile and compressive strain variation in two-way ribbed specimens uniaxially loaded of Series 25. Strain gauges are attached to the centre of the bottom face.

SERIES 30										
f'_c (psi)	P (lbs)	P/f'_c	STRAIN (μin/in) SPECIMEN 30/2		30/4		30/6		AVERAGE STRAIN (in/in)	
	350	0.09	20	-7	18	-8	12	-6	16.7	-7
	850	0.23	36	-14	31	-14	25	-13	30.7	-13.7
	1350	0.36	60	-20	46	-18	40	-20	48.7	-19.3
	1850	0.50	86	-25	62	-25	57	-28	68.3	-26
	2350	0.63	109	-29	78	-30	72	-34	86.3	-31
	2850	0.77	150	-34	98	-38	90	-42	112.7	-38
3720	3350	0.90	192	-38	118	-43	106	-50	138.7	-43.7
	3850	1.03	267	-46	152	-44	119	-60	179.3	-50
	4350	1.17	410	-47	170	-38	132	-69	237.3	-51.3
	4850	1.30		-50	146	-38	250	-79		-55.7
	5350	1.44			134	-38				

TABLE 12 Strain measurements plotted in Fig. 17c

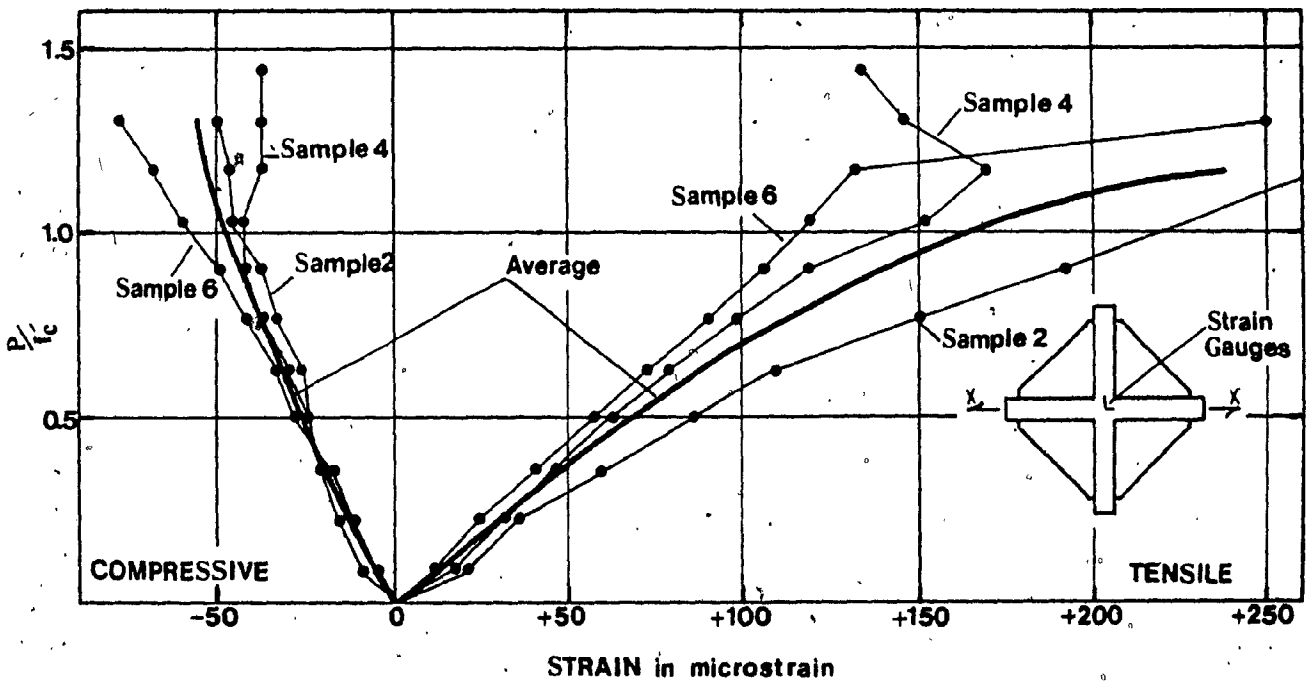

Fig. 17c Tensile and compressive strain variation in two-way ribbed specimens uniaxially loaded of Series 30. Strain gauges are attached to the centre of the bottom face.

SERIES 35											
f'_c (psi)	P (lbs)	P/f'_c	STRAIN (μin/in) SPECIMEN 35/2		35/4		35/6		AVERAGE STRAIN (μin/in)	
	350	0.09	11	-7	18	-8				
	850	0.21	27	-14	29	-12	30	-21	30	-15.7
	1350	0.34	42	-20	44	-17	60	-30	48.7	-22.3
	1850	0.46	60	-28	60	-23	86	-40	68.7	-30.3
4020	2350	0.58	76	-33	74	-28	116	-48	88.7	-36.3
	2850	0.71	95	-38	94	-34	152	-58	113.7	-43.3
	3350	0.83	110	-42	112	-40	200	-68	140.7	-50
	3850	0.96	132	-48	134	-46	252	-70	172.7	-54.7
	4350	1.08	152	-50	141	-54	531	-80	274.7	-61.3
	4850	1.21	169	-57	114	-60	652	-90	311.7	-69
	5350	1.33	180	-62						

TABLE 13 Strain measurements plotted in Fig. 17d

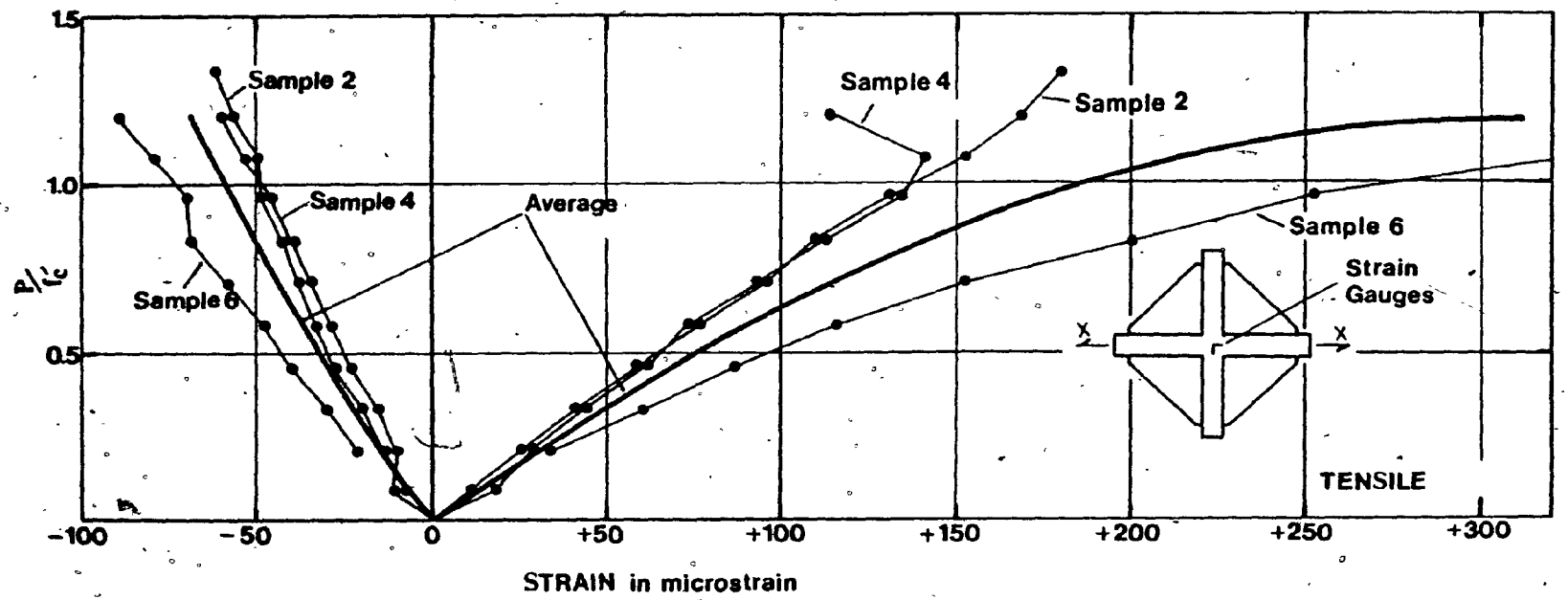

Fig. 17d Tensile and compressive strain variation in two-way ribbed specimens uniaxially loaded of Series 35. Strain gauges ate attached to the centre of the bottom face.

SERIES 30.1										
f'_c (psi)	P (lbs)	P/f'_c	STRAIN (μin/in) SPECIMEN 30.1/1		30.1/2		30.1/3		AVERAGE STRAIN (μin/in)	
	350	0.08	11	-8	11	-4.5	16	-7	12.7	-6.5
	850	0.20	25	-13	28.5	-11	34	-17.5	29.2	-13.8
	1350	0.31	40	-20	41.5	-15.5	55	-26	45.5	-20.5
	1850	0.43	53	-25.5	57	-21	75	-34	61.7	-26.8
4350	2350	0.54	65.5	-30.5	70	-26.5	94.5	-44	76.7	-33.7
	2850	0.66	80.5	-37	87.5	-33	85	-52.5	84.3	-40.8
	3350	0.77	93	-41	102	-39.5	86.5	-62.5	93.8	-47.7
	3850	0.89	103	-45	119	-45	86.5	-71	102.8	-53.7
	4350	1.0	107.5	-47.5	131.5	-51	87	-80	108.7	-59.5
	4850	1.11	34	-49	122	-58.5	105.5	-88	87.2	-65.2

TABLE 14 Strain measurements plotted in Fig. 17e

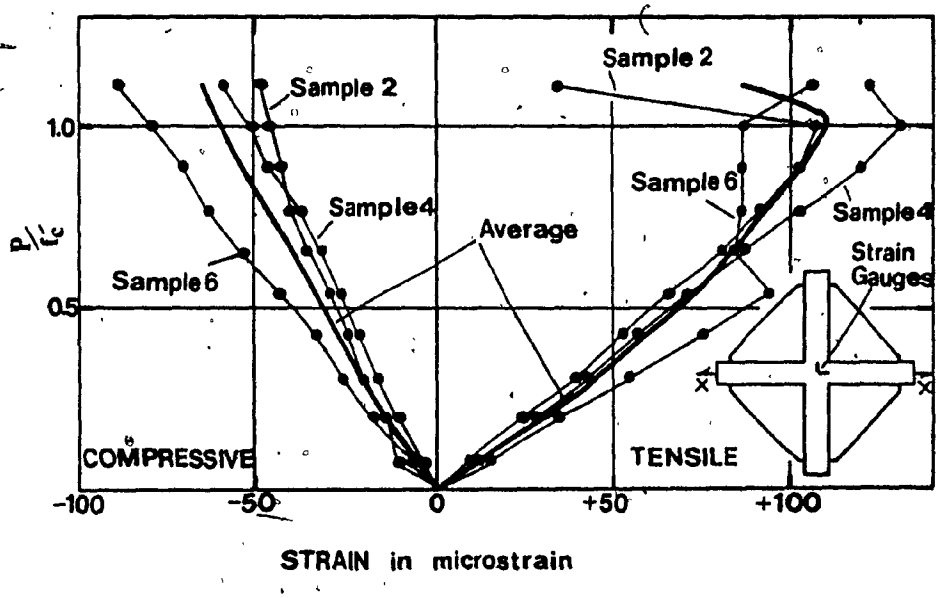

Fig. 17e Tensile and compressive strain variation in two-way ribbed specimens uniaxially loaded of series 30.1. Strain gauges are attached to the centre of the bottom face.

SERIES 30.1						
f'_c (psi)	P (lbs)	P/f'_c	STRAIN (μin/in) SPECIMEN 30.1/4	30.1/5	30.1/6	AVERAGE STRAIN (μin/in)
	375	0.09	10		16	(13)
	875	0.20	19		42	(30.5)
	1375	0.32	27	39.5	60.5	42.3
	1875	0.43	35.5	53	83.5	57.3
	2375	0.55	44.5	64	103	70.5
	2875	0.66	51	78	128.5	85.8
4350	3375	0.78	59	88.5	152.5	100
	3875	0.89	63.5	99	182	114.8
	4375	1.01	68	109.5	209	128.8
	4875	1.12	70	118.5	249	145.8
	5375	1.24	75	127.5	290	164.2
	5875	1.35			560	

TABLE 15 Strain measurements plotted in Fig. 18

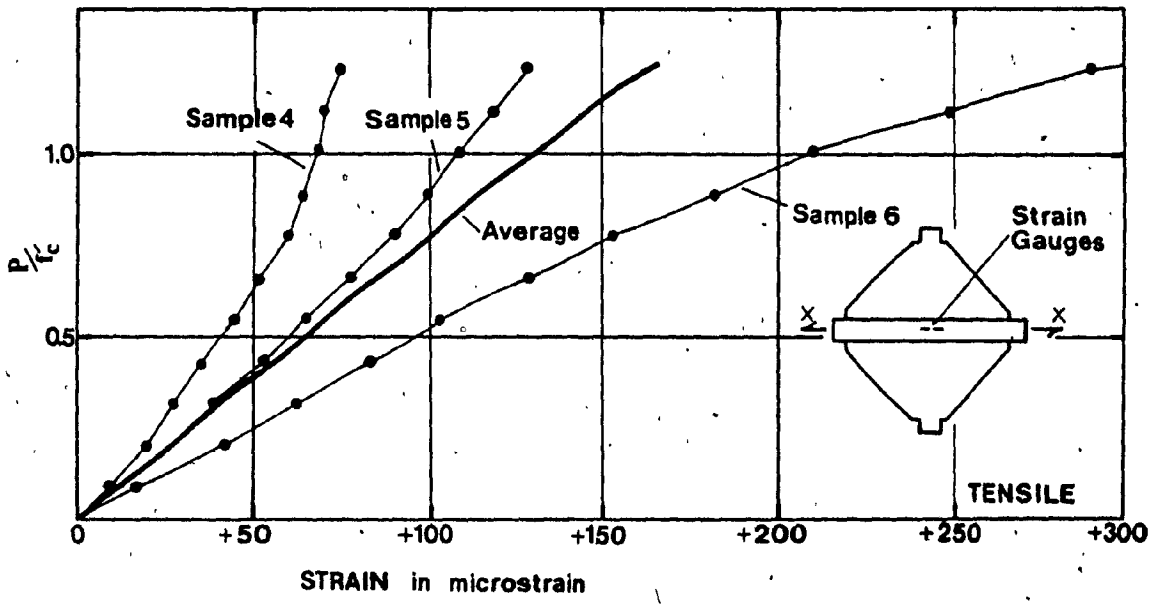

Fig. 18 Tensile strain variation in one-way ribbed specimens of Series 30.1. Strain gauges are attached to the centre of the bottom face.

SERIES 20						
f'_c (psi)	P (lbs)	P/f'_c	STRAIN (μin/in) SPECIMEN 20.2	20.4	20.6	AVERAGE STRAIN (μin/in)
	350	0.10	15	12	15	14
	850	0.25	31	28	29	29.3
	1350	0.39	52	46	45	47.7
3430	1850	0.54	70	60	59	63
	2350	0.69	89	73	74	78.7
	2850	0.83	108	84	86	92.7
	3350	0.98	128	90	99	105.7
	3850	1.12	146		112	(129)
	4350	1.24	173		126	(149.5)

TABLE 16 Strain measurements plotted in Fig. 19a

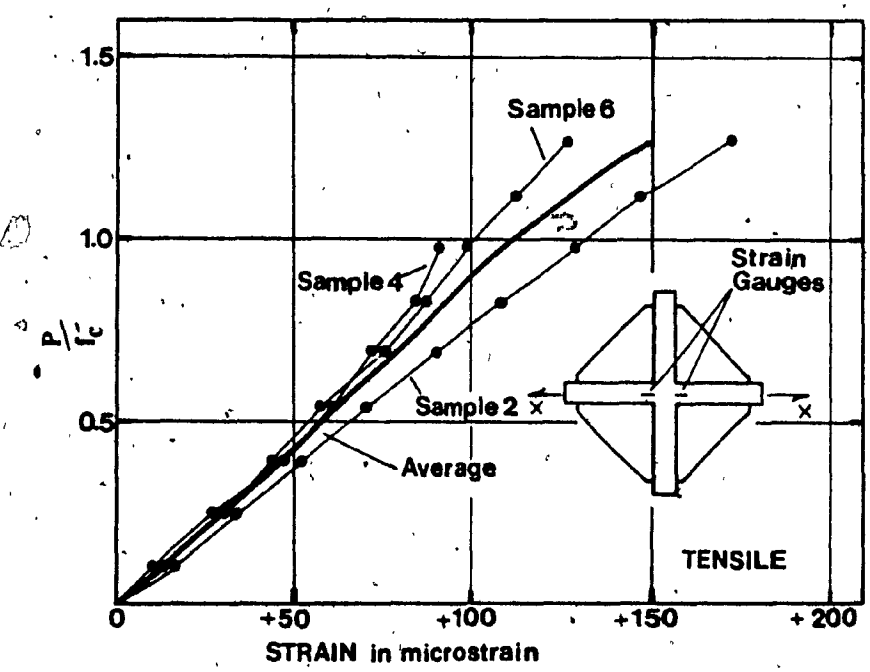

Fig. 19a Tensile strain variation in two-way ribbed specimens uniaxially loaded of Series 20. Strain gauges are attached along the edges of the joint core.

SERIES 30						
f'_c (psi)	P (lbs)	P/f'_c	STRAIN(μin/in) SPECIMEN 30.2	30.4	30.6	AVERAGE STRAIN (μin/in)
	350	0.09	12	16	12	13.3
	850	0.23	26	27	24	25.7
	1350	0.36	36	44	36	38.7
	1850	0.50	52	60	50	54
	2350	0.63	63	72	61	65.3
3720	2850	0.77	77	88	74	79.7
	3350	0.90	89	103	85	92.3
	3850	1.03	105	117	96	106
	4350	1.17	119	142	108	123
	4850	1.30	90	158	124	124
	5350	1.44		172		(172)
	5850	1.57		183		(183)

TABLE 17 Strain measurements plotted in Fig. 19b

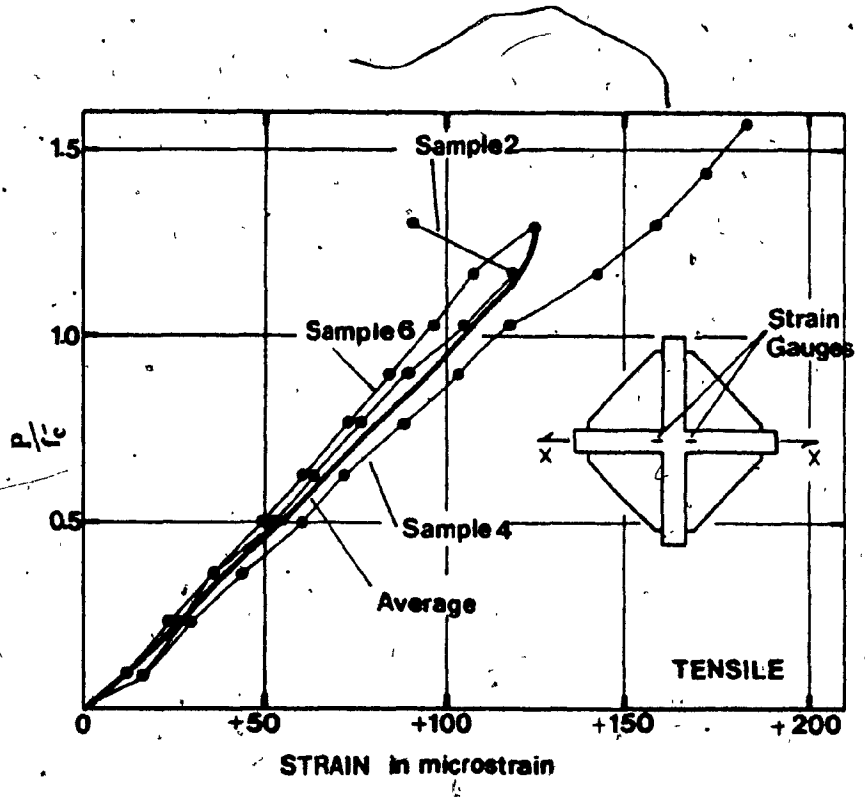

Fig. 19b Tensile strain variation in two-way ribbed specimens uniaixially loaded of series 30. Strain gauges are attached along the edges of the joint core.

SERIES 30.1						
f'_c (psi)	P (lbs)	P/f'_c	STRAIN(μin/in) SPECIMEN 30.1/1	30.1/2	30.1/3	AVERAGE STRAIN (μin/in)
	350	0.08	12	16	11.5	13.2
	850	0.20	21.5	35	24	26.8
	1350	0.31	34	50	36	40
	1850	0.43	46.5	66	47	53.2
	2350	0.54	59	83.5	58	66.8
4350	2850	0.66	73	99.5	70.5	81
	3350	0.77	82	116.5	86	94.8
	3850	0.89	89	137.5	92.5	106.3
	4350	1.0	73	158	83	104.7
	4850	1.11	20	195	80	98.3

TABLE 18 Strain measurements plotted in Fig. 19c

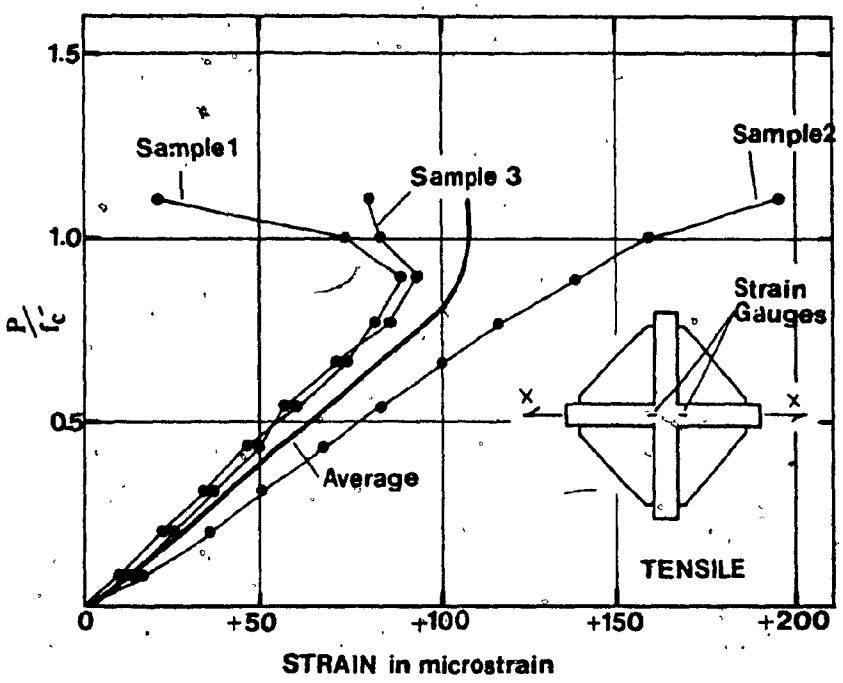

Fig. 19c Tensile strain variation in two-way ribbed specimens uniaxially loaded of series 30.1. Strain gauges are attached along the edges of the joint core.

ANALYSIS OF TEST DATA

Figure 20 shows a section of a plain concrete T-shaped beam under the influence of bending moment M_{cr}, and the stress and strain diagrams. The section of specimen was chosen in such a way that the neutral axis lay in the flange, and full depth of the web was subjected to tension. It is assumed that at the moment of cracking stress is distributed according to elastic behaviour in the compression zone and elasto-plastic in tension, as shown in Fig. 20b.

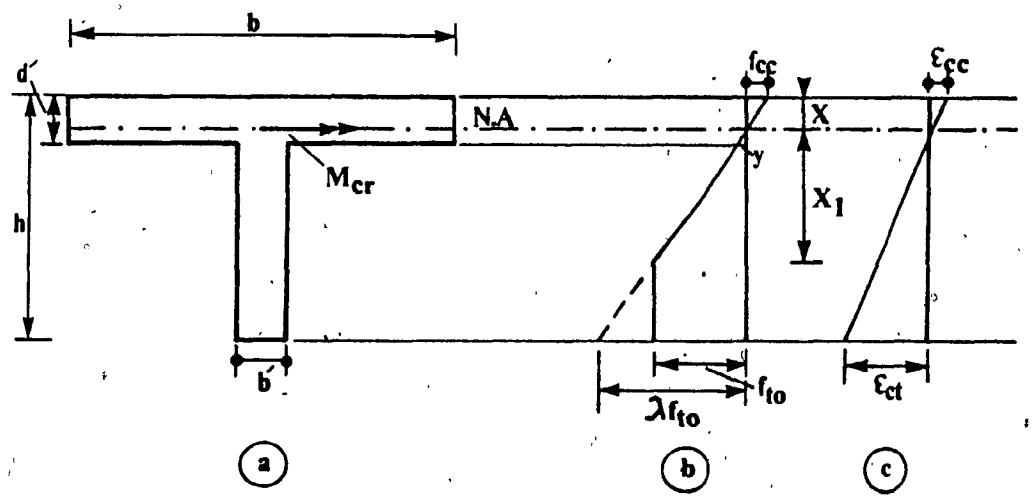

Fig. 20 Cross section of a plain concrete T-shaped beam with stress and strain diagrams

The following relationships can be noted based on Fig. 20b

$$\frac{f_{to}}{\lambda f_{to}} = \frac{x_1}{h-x} \rightarrow x_1 = \frac{1}{\lambda}(h-x) \qquad (1)$$

$$\frac{f_{cc}}{\lambda f_{to}} = \frac{x}{h-x} \rightarrow f_{cc} = \lambda f_{to} \frac{x}{h-x} \qquad (2)$$

From equilibrium of forces and moments $\Sigma P = 0$, $\Sigma M = 0$

we can find:

From

$$\Sigma P=0 \rightarrow \quad \frac{1}{2} f_{cc} x b = \frac{1}{2} f_{to} \frac{(d'-x)^2}{x_1} b + \frac{f_{to} \frac{d'-x}{x_1} + f_{to}}{2} \cdot (x_1+x-d')b' +$$

$$+ f_{to}(h-x-x_1)b'$$

and

$$\kappa(\lambda-1)^2x^2+[2d'\lambda^2(1-\kappa)+2h(2\lambda-1)\kappa]x-[\lambda^2d'^2(1-\kappa)+h^2(2\lambda-1)\kappa]=0 \qquad (3)$$

where $\kappa = \frac{b'}{b}$

Naming

$\kappa(\lambda-1)^2 = \alpha$

$2d'\lambda^2(1-\kappa)+2h(2\lambda-1)\kappa = \beta$

$\lambda^2d'^2(1-\kappa)+h^2(2\lambda-1)\kappa = \gamma$

Equation (3) can be written as

$$\alpha x^2+\beta x-\gamma = 0 \qquad (4)$$

From

$$\Sigma M=0 \rightarrow \quad M_{cr} = \frac{1}{2} f_{cc}\, xb \frac{2x}{3} + \frac{1}{2} f_{to} \frac{(d'-x)^2}{x_1} b \cdot \frac{2}{3}(d'-x) +$$

$$+ \frac{f_{to}+ f_{to} \frac{d'-x}{x_1}}{2} \cdot (x+x_1-d')b' \cdot \left[\frac{(x+x_1-d')}{3} \cdot \frac{f_{to} \frac{d-x}{x_1} + 2f_{to}}{f_{to} \frac{d'-x}{x_1} + f_{to}} + \right.$$

$$\left. + (d'-x)\right] + \frac{1}{2} f_{to}(h-x-x_1)b'(h-x+x_1)$$

and

$$M_{cr} = \frac{1}{6x_1} f_{to} \cdot \left[2x^3b+2(d'-x)^3b+b'(x+x_1-d')^2(d'-x+2x_1)+ \right.$$

$$\left. +3b'(x_1+d'-x)(x+x_1-d')(d'-x)+3b'x_1(h-x-x_1)(h-x+x_1)\right] \qquad (5)$$

Naming

$2x^3b = \delta$

$2(d'-x)^3b = \varepsilon$

$b'(x+x_1-d')^2(d'-x+2x_1) = \zeta$

$3b'(x_1+d'-x)(x+x_1-d')(d'-x) = \theta$

$3b'x_1(h-x-x_1)(h-x+x_1) = \mu$

Equation (5) can be written as

$$M_{cr} = \frac{1}{6x_1} f_{to} (\delta+\varepsilon+\zeta+\vartheta+\mu) \qquad (6)$$

or

$$f_{to} = \frac{6x_1 M_{cr}}{(\delta+\varepsilon+\zeta+\vartheta+\mu)} \qquad (7)$$

From the above equations, it will be possible to establish flexural tensile strength in concrete at failure. For recorded test load at failure P_{cr}, the procedure of calculation consists of the following steps:

1) Calculate moment at failure, M_{cr}
2) Consider a certain value of plasticity factor, λ
3) Apply Eq.(4) to find x
4) Apply Eq.(1) to find x_1

5) Apply Eq.(7) to find f_{to}

Based on the above process (considering λ=1.5), all test data were utilized in the analysis. The results are shown in Table 19.

STRESS-STRAIN RELATIONSHIP

Three cylinders 6x12 in (15x30 cm) were tested in short-time uniaxial compression (Fig. 21) to study the stress-strain relationship. Strain gauges were attached to the cylinders along two diametrically opposed generating lines at mid-height. Measurements of longitudinal strains were carried out and recorded at 10 kips (44.48 kn) load increments. The results are plotted in Fig. 22.

As can be seen, the curve consists of an initial relatively straight portion in which stress and strain are closely proportional. It then begins to curve to the horizontal, reaching the maximum stress f'_c = 3860 psi (26.6 MPa), i.e. the compressive strength, at a strain of 0.00153 in/in.

The secant at 50% of the compressive strength f'_c, considered to represent the modulus of elasticity, gives:

$$E_c = t_{ga} = \frac{0.5(3860)}{610 \times 10^{-6}} = 3.2 \times 10^6 \text{psi (21,850 MPa)}$$

The corresponding value, according to ACI recommended formula, will be:

$$E_c = 33W^{1.5}\sqrt{f'_c} = 33(150)^{1.5}\sqrt{3860} = 3.77 \times 10^6 \text{ (25,970 MPa)}$$

TABLE 19

TEST RESULTS

SERIES NO.	SPECIMEN DESIGNATION	SERIES COMPRESSIVE STRENGTH f'_c	TYPE OF LOADING	TYPE OF SPECIMEN	FORCE AT FAILURE	MAXIMUM STRAIN BEFORE FAILURE (STRAIN GAUGES AT THE CENTRE)		MAXIMUM STRAIN BEFORE FAILURE (STRAIN GAUGES ALONG THE EDGES)		ρ^b_u / ρ_{uu}	CALCULATED FAILURE TENSILE STRESS AT BOTTOM	f_t / f'_c	MODE OF FAILURE
		(psi(MPa)			lbs(KN)	μin/in		μin/in			psi(MPa)		
(1)	(2)	(3)	(4)	(5)	(6)	(7)		(8)		(9)	(10)	(11)	(12)
1	20/1	3430(23.66)	BIAXIAL	TWO-WAY RIBS	7350(32.7)	61	-	-	-	1.0	310.91(2.14)	0.091	Y
	20/3				10850(48.3)	164	-	-	-		458.96(3.17)	0.133	Y
	20/5				8850(39.4)	105	-	-	-		374.36(2.58)	0.109	Y
	20/2		UNIAXIAL		4750(21.1)	135	-68	173	-		401.38(2.77)	0.117	/
	20/4				3850(17.1)	160	-46	90	-		325.33(2.24)	0.095	/
	20/6				4725(21.01)	136	-73	126	-		399.26(2.75)	0.116	/
2	25/1	3830(26.41)	BIAXIAL	TWO-WAY RIBS	8350(37.1)	58	-	-	-	0.7	353.21(2.44)	0.092	/
	25/3				6100(27.1)	53	-	-	-		258.03(1.78)	0.067	/
	25/5				6450(28.7)	48	-	-	-		272.04(1.88)	0.071	/
	25/2		UNIAXIAL		4850(21.6)	340	-43	-	-		409.83(2.83)	0.107	/
	25/4				4600(20.5)	108	-52	-	-		388.70(2.68)	0.101	/
	25/6				5600(24.9)	144	-53	-	-		473.2(3.26)	0.124	/
3	30/1	3720(25.66)	BIAXIAL	TWO-WAY RIBS	8675(38.6)	79.5	-	-	-	0.8	366.95(2.53)	0.099	/
	30/3				9600(42.7)	82.5	-	-	-		406.08(2.80)	0.109	/
	30/5				7725(34.4)	77	-	-	-		326.77(2.55)	0.088	/
	30/2		UNIAXIAL		4925(21.9)	410	-47	119	-		416.16(2.87)	0.112	/
	30/4				5850(26.02)	170	-44	183	-		494.33(3.41)	0.133	/
	30/6				5350(23.8)	250	-79	124	-		452.08(3.12)	0.122	/
4	35/1	4350(30.0)	BIAXIAL	TWO-WAY RIBS	9000(40.03)	62	-	-	-	0.83	380.7(2.63)	0.095	Y
	35/3				9675(43.03)	101	-	-	-		409.25(2.82)	0.102	/
	35/5				7900(35.1)	89.5	-	-	-		334.17(2.3)	0.083	Y
	35/2		UNIAXIAL		5675(25.2)	180	-62	-	-		479.54(3.31)	0.119	/
	35/4				5000(22.2)	141	-60	-	-		422.5(2.91)	0.105	/
	35/6				5350(23.8)	652	-90	-	-		452.08(3.12)	0.112	/
5	30.1/1	4350(30.0)	UNIAXIAL	TWO-WAY RIBS	4850(21.6)	107.5	-49	89	-16	-	409.83(2.83)	0.094	/
	30.1/2				5350(23.8)	131.5	-58.5	195	-		452.08(3.12)	0.104	/
	30.1/3				4975(22.1)	105.5	-88	92.5	-		420.39(2.90)	0.097	/
	30.1/4			ONE-WAY RIBS	5825(25.9)	75	-	126	-		492.21(3.39)	0.113	/
	30.1/5				5750(25.6)	127.5	-	84			485.88(3.35)	0.112	/
	30.1/6				6375(28.4)	560	-	174	-		538.69(3.72)	0.124	/

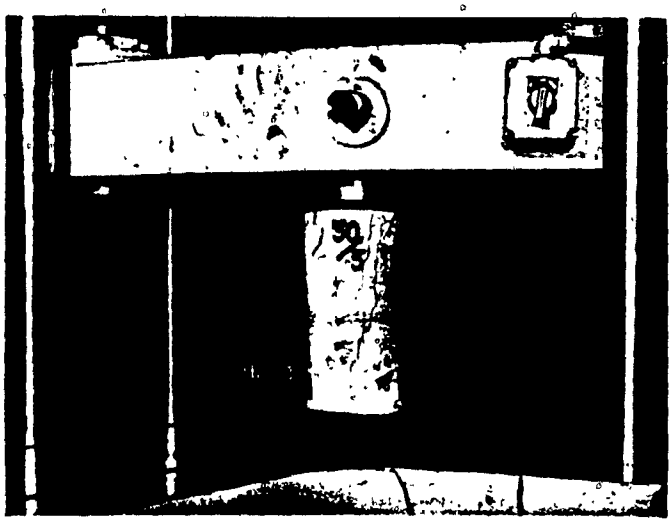

Fig. 21a Cylinder in testing

Fig. 21b Crack patterns in cylinders after failure

DATA FOR THE STRESS-STRAIN CURVE				
P (lbs)	COMPRESSIVE STRESS f'_c (psi)	AVERAGE COMPRESSIVE STRAIN (μin/in) CYLINDER		
		30/1	30/2	30/3
10,000	354	-138	-99	-56
20,000	707	-268	-323	-128
30,000	1061	-404	-483	-203
40,000	1415	-546	-631	-280
50,000	1768	-695	-750	-368
60,000	2122	-846	-880	-461
70,000	2476	-994	-994	-566
80,000	2829	-1152	-1143	-688
90,000	3183	-1327	-1371	-824
100,000	3537	-1530		-986
110,000	3890			-1192

TABLE 20 Compressive strain measurements plotted in Fig. 22.

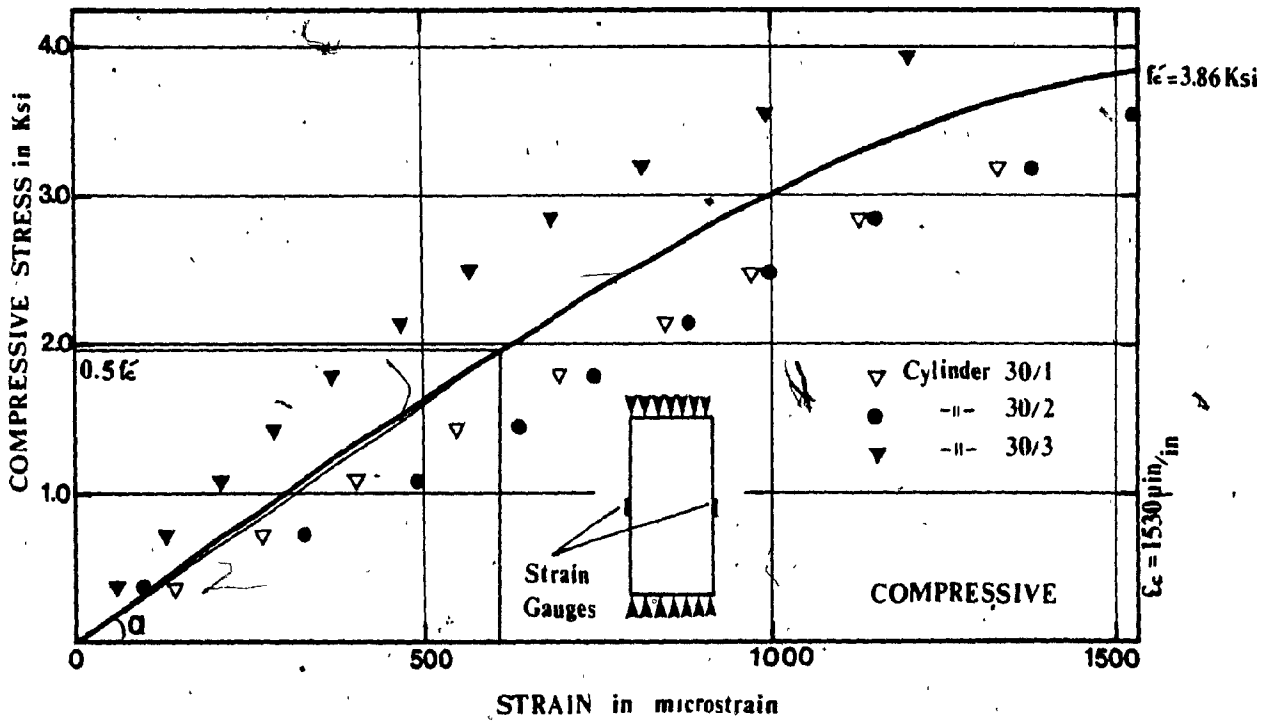

Fig. 22 Concrete stress-strain variation in compression

COMPARISON OF SPLIT-CYLINDER TEST RESULTS WITH THOSE OBTAINED FROM TESTING OF SPECIMENS

In split-cylinder test, the loading condition represents a special case of the biaxial stress state in which the cylinder is under compression f_{ct} and simultaneous tension f_t' where $f_{ct} = 3f_t'$ (if it is calculated on the basis of the theory of elasticity as is usually done). (Fig.23). If a linear function is to be assumed for f_{tc} [2,3,4,5,6,7,8,9] (strength of concrete under combined bi-directional tension and compression) as presented in the diagram in Fig. 24, and $f_t' = 0.0915\ f_c'$ (based on test results shown in Table 3), then the pure tensile strength of concrete can be defined as $f_{to} = 0.1261\ f_c'$ and consequently $f_t' = 0.7256\ f_{to}$. This means that the uniaxial tensile strength of concrete is approximately $\frac{1}{0.7256} = 1.378$ of tensile strength as defined by splitting of cylinders.

Using the above relationship between f_t' and f_{to}, split-cylinder test results are transferred to pure tensile strength of concrete and are compared with those obtained from testing of specimens, as shown in Table 21.

On the basis of this comparison, it can be stated that the used value of $\lambda = 1.5$ as the plasticity factor for calculating tensile strength of specimens is correct (for concrete strengths ranging from 3720 psi (25.66 MPa) to 4350 psi (30.0 MPa)).

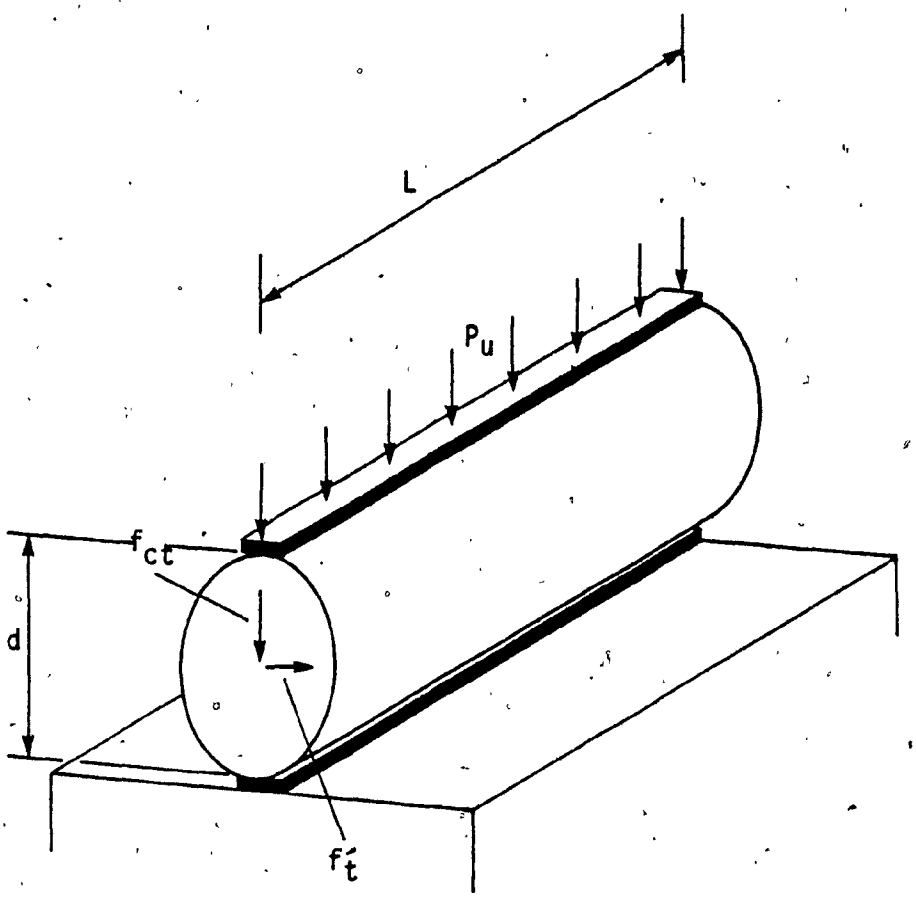

Fig. 23 Split-cylinder test where $f_{ct} = 3f'_t$ and $f'_t = \frac{2P_u}{\pi dL}$

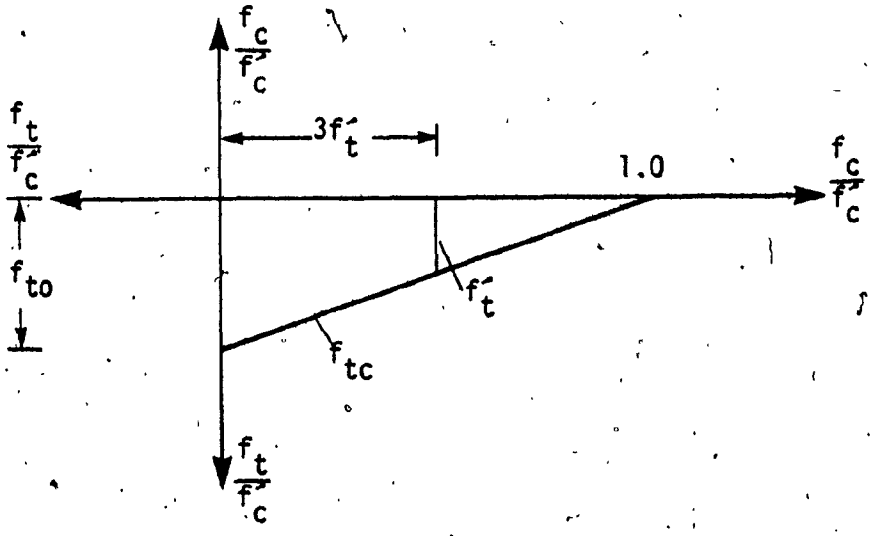

Fig. 24 Strength envelope of concrete under biaxial tension stress state

TABLE 21. COMPARISON OF SPLIT-CYLINDER TEST RESULTS WITH THOSE OBTAINED FROM TESTING OF SPECIMENS

SERIES NO.	CYLINDER DESIGNATION	CYLINDER LENGTH L	LOAD AT SPLITTING P_u	STRESS* AT SPLITTING f'_t	$\frac{f'_t}{0.7256} = f_{to}$	AVERAGE OF f_{to}	AVERAGE OF f_{to} FROM TESTING OF SPECIMENS
		in(mm)	lbs(KN)	psi(MPa)	psi(KN)	psi(KN)	psi(KN)
(1)	(2)	(3)	(4)	(5)	(6)	(7)	(8)
3	30/1	7.0(177.8)	25,625(114.0)	388(2.7)	534.7(3.7)	537.25(3.7)	535.9(3.7)
	30/2	6.75(171.5)	22,500(100.1)	354(2.4)	487.9(3.4)		
	30/3	6.75(171.5)	23,500(104.6)	370(2.6)	509.9(3.5)		
	30/4	6.75(171.5)	26,250(116.8)	413(2.8)	569.2(3.9)		
	30/5	6.125(155.6)	23,000(102.3)	398(2.7)	548.5(3.8)		
	30/6	6.0(152.4)	23,500(104.6)	416(2.9)	575.3(4.0)		
5	30.1/1	6.75(171.5)	17,425(77.5)	274(1.9)	377.6(2.6)	470.4(3.2)	505.6(3.5)
	30.1/2	6.875(174.6)	22,275(99.1)	343(2.4)	472.7(3.3)		
	30.1/3	6.625(168.3)	25,425(113.1)	407(2.8)	560.9(3.9)		

* STRESS AT SPLITTING f_{to} IS CALCULATED USING THE FORMULA $f'_t = \frac{2P_u}{\pi dL}$

BIAXIAL STRENGTH ENVELOPE

All relative failure loads P_u for uniaxial and biaxial loading conditions have been plotted in Fig. 25a as fractions of the uniaxial compressive strength of concrete. It can be seen that the ratio P_u^b/P_u^u of the average load at failure in biaxial loading to the average failure load in uniaxial loading equals 0.73.

A similar ratio can be seen in Fig. 25b where all tensile stresses at failure for uniaxial and biaxial loading have been plotted as fractions of the uniaxial compressive strength of concrete.

It can be stated on the basis of the results presented here that the flexural tensile strength of concrete subjected to equal biaxial stress states is about 73% of the uniaxial tensile strength or, stated otherwise, the uniaxial tensile strength of concrete is about 37% higher than the biaxial. This observation may be significant, and can not be ignored in the design of structures such as atomic reactor vaults and pressure vessels which are subjected to the biaxial stress state and where no cracks are permitted.

Fig. 26 shows a proposed biaxial strength envelope of concrete under all load combinations, i.e. compression-compression, compression-tension and tension-tension, to be used in engineering practice. Under combined compression-compression, strength increases linearly up to 25% of uniaxial strength f_c'. Under combined compression-tension, the compressive strength decreases linearly as the tensile stress is increased. Eventually, under combined tension-tension, strength decreases in comparison with uniaxial tensile strength and in equal biaxial tension strength particularly is approximately 70% of uniaxial tension.

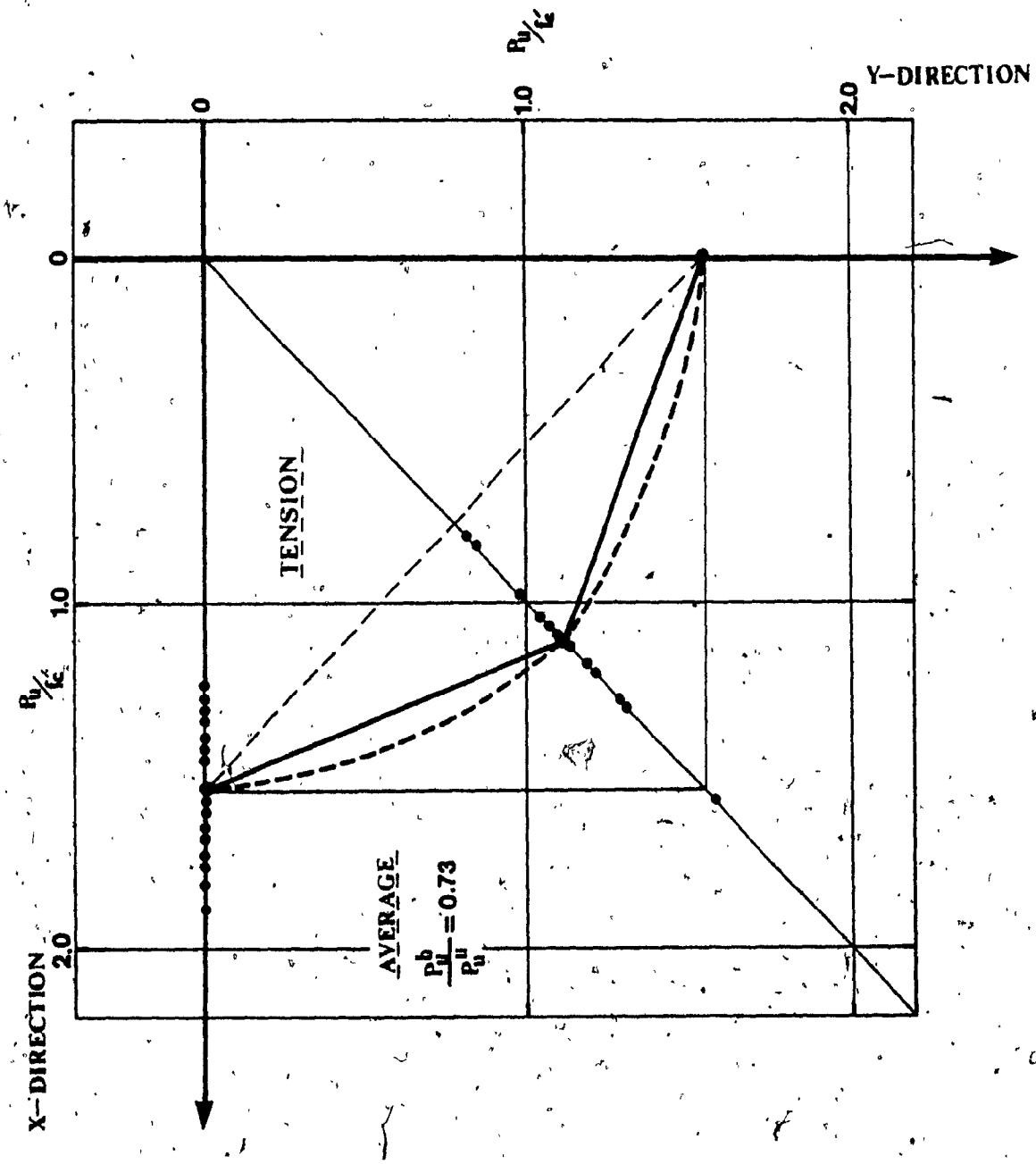

Fig. 25a Proposed ultimate strength envelope of concrete under biaxial tension stress state.

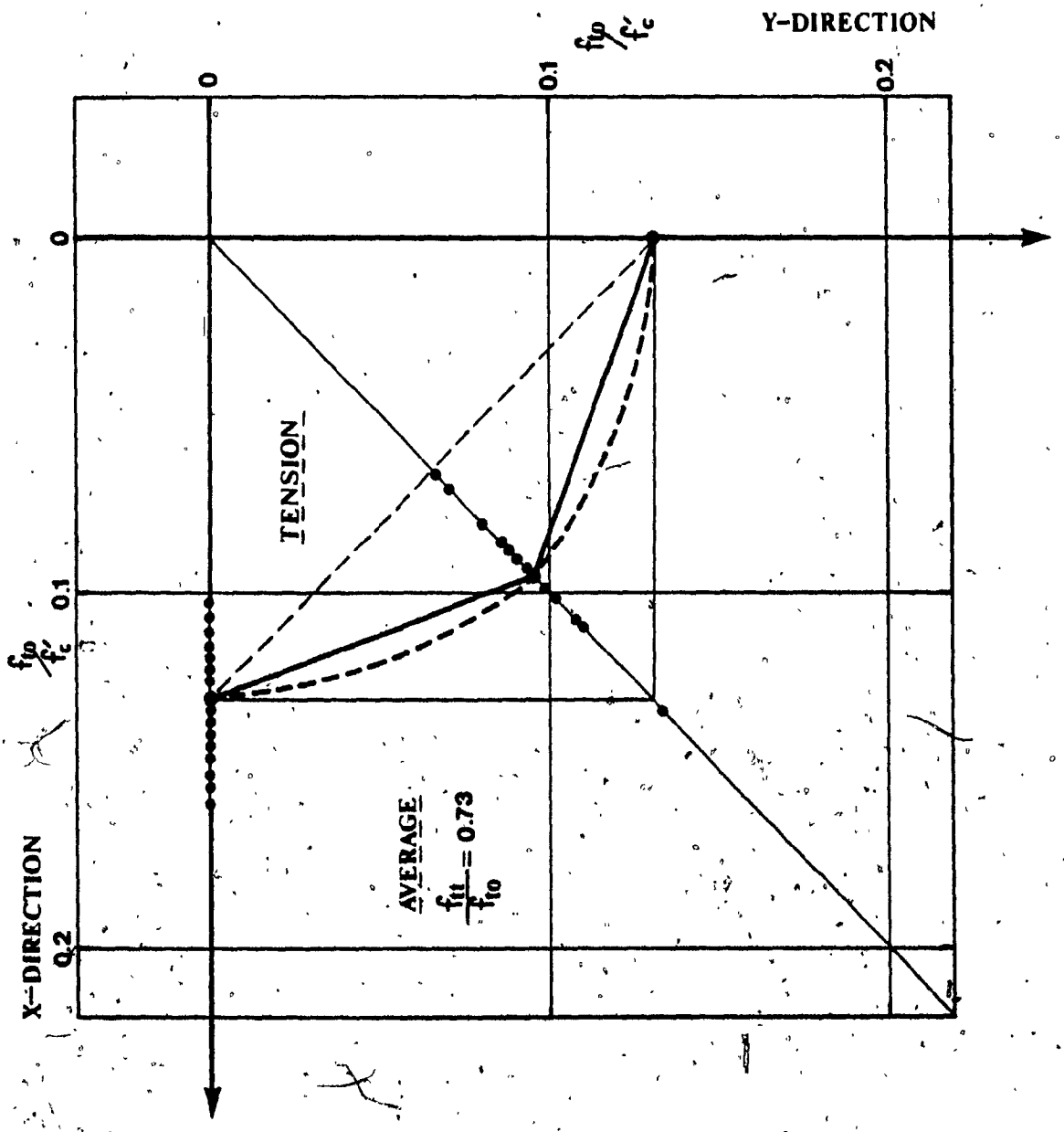

Fig. 25b Proposed ultimate strength envelope of concrete under biaxial stress state

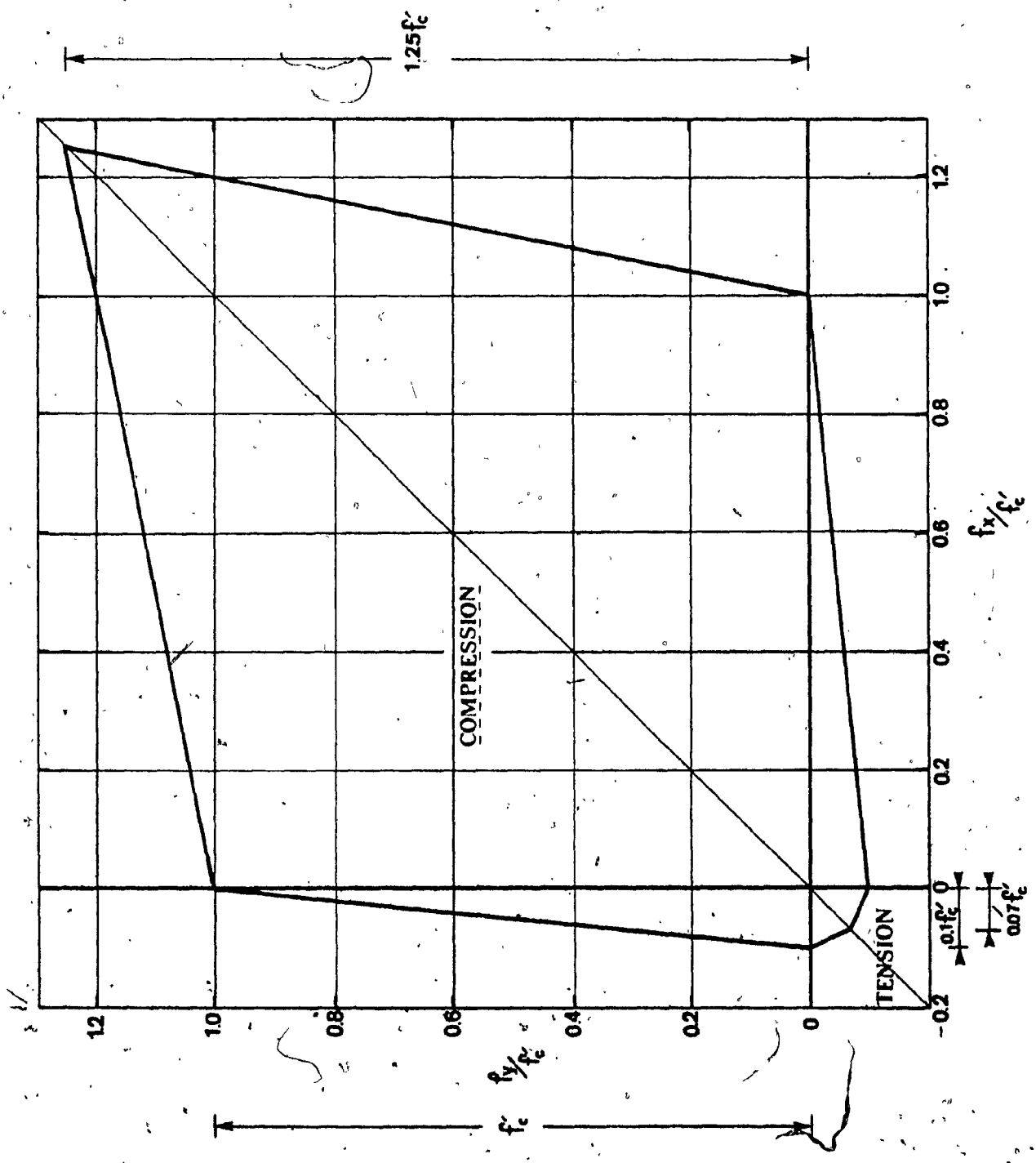

Fig. 26 Proposed overall biaxial ultimate strength envelope

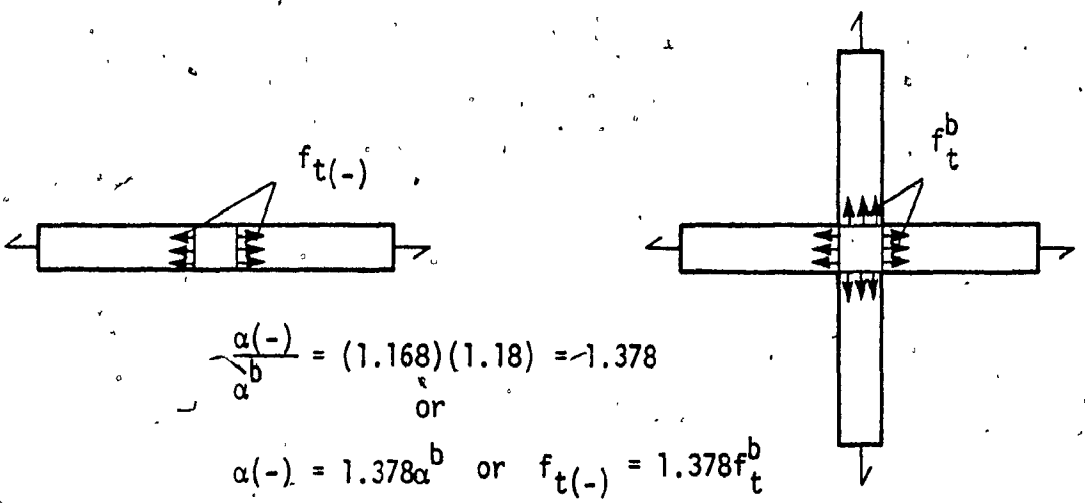

$$\frac{\alpha(-)}{\alpha^b} = (1.168)(1.18) = 1.378$$

or

$$\alpha(-) = 1.378\alpha^b \quad \text{or} \quad f_{t(-)} = 1.378 f_t^b$$

(a)

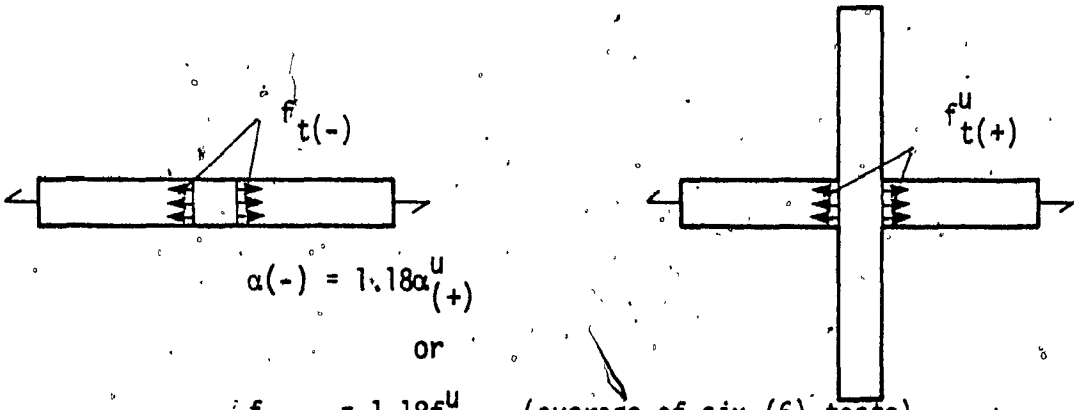

$$\alpha(-) = 1.18\alpha^u_{(+)}$$

or

$$f_{t(-)} = 1.18 f^u_{t(+)} \quad \text{(average of six (6) tests)}$$

(b)

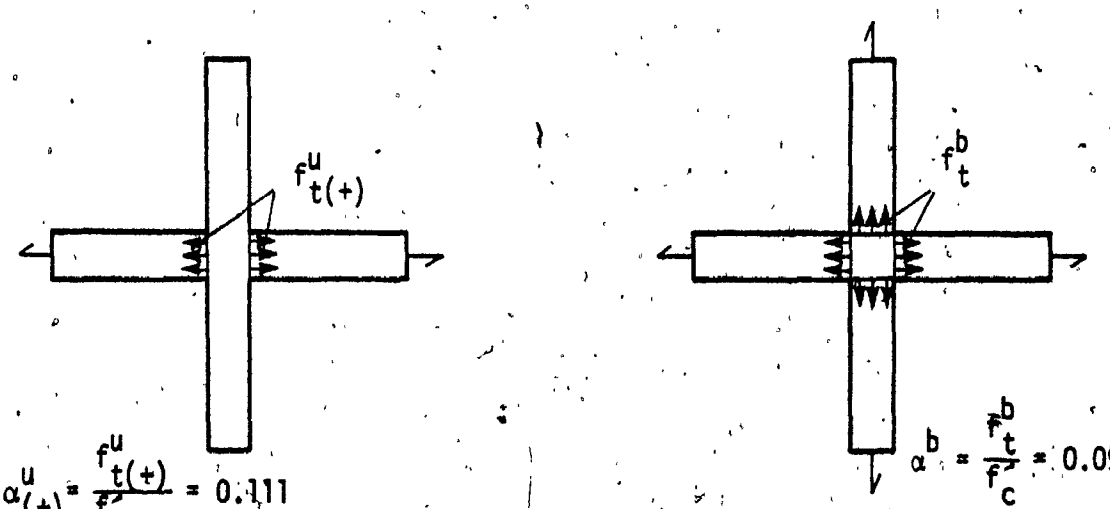

$$\alpha^u_{(+)} = \frac{f^u_{t(+)}}{f'_c} = 0.111$$

(average of 15 tests)

$$\alpha^b = \frac{f_t^b}{f'_c} = 0.095$$

(average of 12 tests)

$$\frac{\alpha^u_{(+)}}{\alpha^b} = \frac{0.111}{0.095} = 1.168 \quad \text{or} \quad \alpha^u_{(+)} = 1.168\alpha^b \quad \text{or} \quad f^u_{t(+)} = 1.168 f_t^b$$

(c)

DISCUSSION OF TEST RESULTS

The results obtained are summarized in Fig. 27 which shows ratios $\alpha = \frac{f_t}{f'_c}$ of relative tensile stress f_t to uniaxial compressive strength f'_c as compared for uniaxial and biaxial loading in one-way and two-way specimens.

Test results show that the flexural tensile strength of concrete in the biaxial stress state is lower than in the uniaxial stress state.

Figure 27a reveals the fact that the uniaxial tensile strength of concrete is about 37% higher than the biaxial. It should be remembered here that our results refer only to a particular case of biaxial strength when stresses in both directions are equal.

It can be seen from Fig. 27b that uniaxial tensile strength in elements with attached cross ribs (two-way system) is about 18% lower than in elements with one rib (one-way system - without cross ribs). Figure 27c shows that in two-way ribbed specimens, uniaxial tensile strength is 16.8% higher than biaxial tensile strength.

CONCLUSIONS

The following conclusions are based on the experimental work in this study:

1. The flexural tensile strength of concrete in the uniaxial stress state is about 37% higher than in the biaxial stress state. The results refer only to a particular case of biaxial strength in which stresses in both directions are equal.
2. The uniaxial tensile strength in elements with attached cross ribs

(two-way system) is about 18% lower than in elements with one rib (one-way system).

3. In two-way ribbed specimens, uniaxial tensile strength is 16.8% higher than biaxial tensile strength.
4. Tensile strain in biaxial loading is approximately one-third of the tensile strain in uniaxial loading.
5. In one-way and two-way ribbed specimens, both tested uniaxially, tensile strains are approximately equal.
6. In two-way specimens tested uniaxially, compressive strain, developed in the free rib, is nearly one-third of the tensile strain.